

Calhoun: The NPS Institutional Archive
DSpace Repository

Theses and Dissertations

Thesis and Dissertation Collection

1976

Theoretical analysis of a model for a field displacement isolator.

Sharon, Ram

Monterey, California. Naval Postgraduate School

<http://hdl.handle.net/10945/17975>

Downloaded from NPS Archive: Calhoun



Calhoun is a project of the Dudley Knox Library at NPS, furthering the precepts and goals of open government and government transparency. All information contained herein has been approved for release by the NPS Public Affairs Officer.

Dudley Knox Library / Naval Postgraduate School
411 Dyer Road / 1 University Circle
Monterey, California USA 93943

<http://www.nps.edu/library>

THEORETICAL ANALYSIS OF A MODEL
FOR
A FIELD DISPLACEMENT ISOLATOR

Ram Sharon

NAVAL POSTGRADUATE SCHOOL

Monterey, California



THESIS

Theoretical Analysis of a Model
for
a Field Displacement Isolator

by

Ram Sharon

June 1976

Thesis Advisor:

J. B. Knorr

Approved for public release; distribution unlimited.

T175032

REPORT DOCUMENTATION PAGE		READ INSTRUCTIONS BEFORE COMPLETING FORM	
1. REPORT NUMBER	2. GOVT ACCESSION NO.	3. RECIPIENT'S CATALOG NUMBER	
4. TITLE (and Subtitle) Theoretical Analysis of a Model for a Field Displacement Isolator		5. TYPE OF REPORT & PERIOD COVERED Electrical Engineer June 1976	
		6. PERFORMING ORG. REPORT NUMBER	
7. AUTHOR(s) Ram Sharon		8. CONTRACT OR GRANT NUMBER(s)	
9. PERFORMING ORGANIZATION NAME AND ADDRESS Naval Postgraduate School Monterey, CA 93940		10. PROGRAM ELEMENT, PROJECT, TASK AREA & WORK UNIT NUMBERS	
11. CONTROLLING OFFICE NAME AND ADDRESS Naval Postgraduate School Monterey, CA 93940		12. REPORT DATE June 1976	
		13. NUMBER OF PAGES 80	
14. MONITORING AGENCY NAME & ADDRESS (if different from Controlling Office) Naval Postgraduate School Monterey, CA 93940		15. SECURITY CLASS. (of this report) UNCLASSIFIED	
		15a. DECLASSIFICATION/DOWNGRADING SCHEDULE	
16. DISTRIBUTION STATEMENT (of this Report) Approved for public release; distribution unlimited.			
17. DISTRIBUTION STATEMENT (of the abstract entered in Block 20, if different from Report)			
18. SUPPLEMENTARY NOTES			
19. KEY WORDS (Continue on reverse side if necessary and identify by block number) Dielectric substrate Ferrite substrate Spectral domain Edge-guided mode			
20. ABSTRACT (Continue on reverse side if necessary and identify by block number) A frequency dependent analysis of a shielded edge-guided mode isolator is presented. A Fourier transform technique is applied to the boundary expressions of a structure built on a dielectric substrate, and the resulting equations are solved for the wavelength ratio. By using perturbation analysis and the results obtained for the dielectric case, solutions for the			

20. Abstract (continued)

normalized propagation constant and attenuation for waves traveling in the -Z and +Z directions, in a structure built on a ferrite substrate, are obtained.

Theoretical Analysis of a Model
for
a Field Displacement Isolator

by

Ram Sharon

Lieutenant Junior Grade, Israeli Navy

B.S.E.E., 'Technion' High Technological Institute, Israel, 1972

M.S.E.E. (with distinc.), Naval Postgraduate School, 1975

Submitted in partial fulfillment of the
requirements for the degree

ELECTRICAL ENGINEER

from the

NAVAL POSTGRADUATE SCHOOL
June 1976

ABSTRACT

A frequency dependent analysis of a shielded edge-guided mode isolator is presented. A Fourier transform technique is applied to the boundary expressions of a structure built on a dielectric substrate, and the resulting equations are solved for the wavelength ratio. By using perturbation analysis and the results obtained for the dielectric case, solutions for the normalized propagation constant and attenuation for waves traveling in the $-Z$ and $+Z$ directions, in a structure built on a ferrite substrate, are obtained.

TABLE OF CONTENTS

I.	INTRODUCTION -----	7
II.	DISPERSION CHARACTERISTICS ON DIELECTRIC SUBSTRATE-----	13
	A. FIELD AND BOUNDARY CONDITIONS -----	13
	B. SPECTRAL DOMAIN TRANSFORM -----	17
	C. DETERMINENTAL EQUATION -----	28
	D. CURRENT DENSITY COMPONENTS -----	32
	E. AVERAGE POWER FLOW -----	36
III.	PERTURBATION ANALYSIS OF EDGE-GUIDED MODE ISOLATOR ON FERRITE SUBSTRATE -----	47
	A. PERTURBATION EXPRESSION FOR PROPAGATION CONSTANT -----	47
	B. MAGNETIC SUSCEPTIBILITY TENSOR ELEMENTS -----	51
	C. COMPUTATION OF PERTURBATION EXPRESSION IN THE SPECTRAL DOMAIN -----	53
	D. COMPUTATION OF NORMALIZED PHASE CONSTANT AND ATTENUATION -----	55
IV.	COMPUTER PROGRAMMING -----	61
V.	CONCLUSIONS -----	64
APPENDIX A:	AVERAGE POWER FLOW IN REGIONS 1 AND 2 -----	65
APPENDIX B:	NORMALIZED PHASE CONSTANT AND ATTENUATION (FOR FERRITE CASE) -----	68
APPENDIX C:	COMPUTER PROGRAM -----	72
LIST OF REFERENCES	-----	79
INITIAL DISTRIBUTION LIST	-----	80

LIST OF FIGURES

1.	R.F. Fields of Dominant Mode in Microstrip Line. D.C. Magnetic Field in -y Direction -----	8
2.	Isolator Structure -----	10
3.	Three Dimensional Isolator and Regions -----	12
4.	Longitudinal and Transverse Current Density Components -----	33
5.	Ratio Between the Two Maxima of the Longitudinal and Transverse Current Density Components -----	34
6.	Computed and Measured Dispersion Characteristics for $D = 0.025''$ $W = 0.45''$ and $D = 0.125''$ $W = 0.45''$ with $\epsilon_r = 16$ -----	37
7.	Average Power Distribution in Region 1 Vs. n (αn) for $f = 4\text{GHz}$, $D = .125''$, $W = 0.45''$, $\epsilon_r = 16$ -----	43
8.	Average Power Distribution in Region 2 vs. n (αn), for $f = 4\text{GHz}$, $D = 0.125''$, $W = 0.45''$, $\epsilon_r = 16$ -----	44
9.	Average Power Ratio in Regions 1 and 2 Vs. Frequency for $\epsilon_r = 9$ -----	45
10.	Average Power Ratio in Regions 1 and 2 Vs. Frequency for $\epsilon_r = 16$ -----	46
11.	Shielded Isolator Structure -----	49
12.	a) Attenuation and b) Normalized Propagation Constant for Waves Traveling in +Z and -Z Directions for: $\Delta H = 75\text{oe}$, $H_{D.C} = 1916.3\text{ oe}$, $4\pi\text{MS} = 1200\text{ Ga}$, $g = 1.99$ $\epsilon_r = 15.2$ -----	56
13.	a) Attenuation and b) Normalized Propagation Constant for Waves Traveling in +Z and -Z Directions for: $\Delta H = 75\text{ oe}$, $H_{D.C} = 2271.42\text{ oe}$, $4\pi\text{MS} = 1200\text{ Ga}$ $g = 1.99$, $\epsilon_r = 15.2$ -----	57
14.	a) Attenuation and b) Normalized Propagation Constant for Waves Traveling in +Z and -Z Directions for: $\Delta H = 75\text{ oe}$, $H_{D.C} = 2628.6\text{ oe}$, $4\pi\text{MS} = 1200\text{ Ga}$, $g = 1.99$, $\epsilon_r = 15.2$ -----	58
15.	Waveguide Filled With Dielectric Slab Perpendicular to the Electric Field -----	63

I. INTRODUCTION

The analysis of various configurations of microstrip transmission lines, is of great importance, primarily, to the industrial area, since these kinds of transmission lines are easy to manufacture, and they are suitable for use in microwave integrated circuits due to their small dimensions.

Two major groups of microstrip transmission lines can be defined, related to the substrate material that is used. These are the dielectric and ferrite substrate groups. This study presents the analysis of a new type of ferrite built, shielded microstrip isolator, using the edge-guided mode of propagation.

It was shown by M. E. Hines [Ref. 1] that an edge-guided mode of propagation occurs in a wide microstrip transmission line using a ferrite slab magnetized perpendicular to the ground plane. The R. F. fields patterns in such a structure are shown in Figure 1 [Ref. 1].

Propagation occurs in both $\pm Z$ directions with equal phase velocities and loss, and the R. F. fields patterns are mirror images for both directions of propagation. In the dominant mode the energy is shifted from one side to the other with reversal of the direction of propagation. Hines suggested that this phenomenon could be used in the analysis of nonreciprocal devices such as isolators, phase shifters

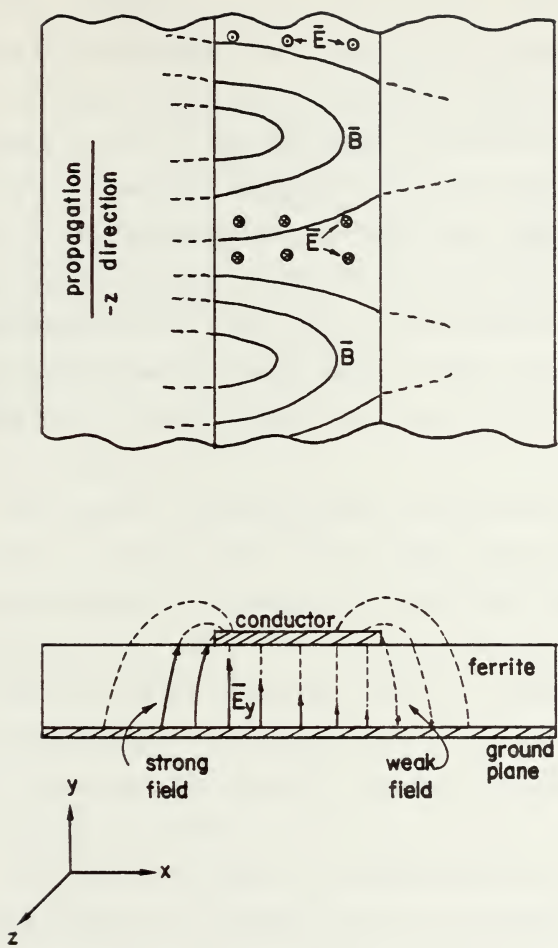


Figure 1. R.F. Fields of Dominant Mode in Microstrip Line. D.C. Magnetic Field in -y Direction.

and other components, where nonreciprocal behavior can be attained by perturbing the structure in an asymmetrical way.

To achieve isolation, a resistive load can be placed only on one side of the structure; thus high transmission loss occurs for the propagation direction for which the energy is concentrated on the lossy side, and lower loss results for the opposite direction where the energy is concentrated on the other side. The disadvantage of this field displacement isolator was the small ratio between backward and forward losses, which was not sufficient for isolation purposes.

An improved edge-guided mode isolator was suggested by K. Araki, T. Koyama and Y. Naito [Ref. 2] for which no lossy electric material was used, but instead one edge of the conducting strip was shorted to ground.

This isolation structure, shown in Figure 2, was built and tested and the experimental result showed large attenuation in the backward direction and small insertion loss in the forward direction.

The following study is an investigation of the theoretical behavior of a model for this isolator structure.

The exact configuration of the isolator model is shown in Figure 3. Since most of the field is confined in the dielectric substrate then the left, right and upper conducting walls of the shield have negligible affect on the electric and magnetic fields configuration, thus the model which is

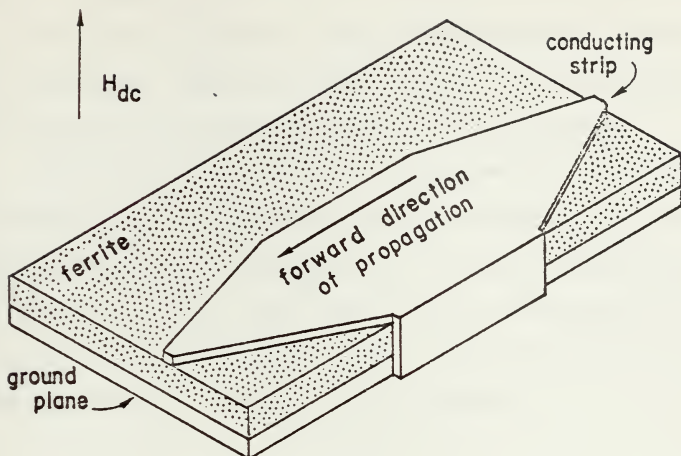


Figure 2. Isolator Structure.

easier to analyze can replace the open boundary-isolator configuration [Figure 2]. The shield is a rectangular waveguide which implies that the highest frequency of operation should not exceed the cut-off frequency of the TE_{10} mode of the waveguide.

The mathematical method which was selected for this study was used in earlier works like references 3, 4, and 5. This mathematical method can be used for calculating wavelength ratio and characteristic impedance for non TEM, TE or TM transmission lines. Essentially, this method deals with the boundary conditions of a structure, after they were transformed into the spectral domain. Then by using the

method of moment [Ref. 4] and assuming either current density distributions or electric field distributions (depending on the structure) numerical solutions for the wavelength ratio and the characteristic impedance can be obtained.

In essence, the analysis procedure is a complete solution for the dispersion characteristics of a structure built on a dielectric substrate, and then by applying perturbation theory, the phase and the attenuation constants of a structure built on a ferrite substrate are obtained. This ferrite built device is the isolator.

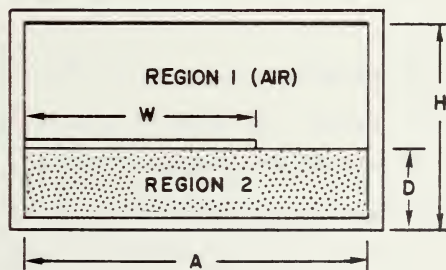
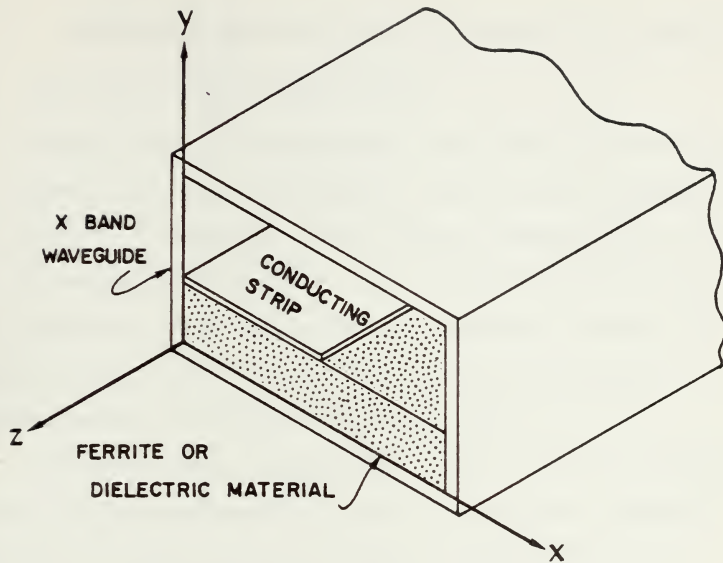


Figure 3. Three dimensional Isolator and Regions.

II. DISPERSION CHARACTERISTICS ON DIELECTRIC SUBSTRATE

A. FIELD AND BOUNDARY CONDITIONS

Assume waves are propagating along the structure shown in Figure 3, in the $-Z$ direction such that the propagation term is $e^{j\omega t + \gamma Z}$ where ω is the radian frequency, and $\gamma = \alpha + j\beta$ is the propagation constant. We assume from now on that for the dielectric substrate γ is pure imaginary, hence $\alpha = 0$. Later we shall see that for the ferrite substrate, γ is a complex number including both terms α and β .

The longitudinal components of the electric and magnetic fields can be expressed in terms of the scalar electric potential ϕ^e and the scalar magnetic potential ϕ^h as

$$Ez_i = Kc_i^2 \phi_i^e(x,y)e^{\gamma Z} \quad (1)$$

$$Hz_i = Kc_i^2 \phi_i^h(x,y)e^{\gamma Z} \quad (2)$$

where $Kc_i^2 = K_i^2 + \gamma^2$ $i = 1,2$ defining the spatial regions of the structure (Figure 3). Using the two field expressions (1) and (2) together with Maxwell's curl equations leads to the transverse components of the electric and magnetic fields as follows:

$$E_{x_i} = \left(\gamma \frac{\partial \phi_i^e}{\partial x} - j\omega\mu_i \frac{\partial \phi_i^h}{\partial y} \right) e^{\gamma z} \quad (3)$$

$$H_{x_i} = \left(\gamma \frac{\partial \phi_i^h}{\partial x} + j\omega\epsilon_i \frac{\partial \phi_i^e}{\partial y} \right) e^{\gamma z} \quad (4)$$

$$E_{y_i} = \left(\gamma \frac{\partial \phi_i^e}{\partial y} + j\omega\mu_i \frac{\partial \phi_i^h}{\partial x} \right) e^{\gamma z} \quad (5)$$

$$H_{y_i} = \left(\gamma \frac{\partial \phi_i^h}{\partial y} - j\omega\epsilon_i \frac{\partial \phi_i^e}{\partial x} \right) e^{\gamma z} \quad (6)$$

$$i = 1, 2.$$

Applying boundary conditions at the interface between the dielectric substrate and the bottom wall of the waveguide ($y=0$), and assuming perfect conducting walls, tangential electric fields should be zero or explicitly writing

$$E_{x_2}(x, 0, z) = 0 \quad (7)$$

$$E_{z_2}(x, 0, z) = 0. \quad (8)$$

At the interface between regions 1 and 2, ($y=D$) the tangential electric field must be continuous:

$$E_{x_1}(x, D, z) = E_{x_2}(x, D, z) \quad (9)$$

$$E_{z_1}(x, D, z) = E_{z_2}(x, D, z). \quad (10)$$

The electric fields at the interface between regions 1 and 2 exist only in the dielectric portion of the interface and can be written as:

$$E_{x_1}(x, D, z) = \begin{cases} 0 & \text{on strip} \\ e_x(x)e^{\gamma z} & W < X < A \end{cases} \quad (11)$$

$$E_{z_1}(x, D, z) = \begin{cases} 0 & \text{on strip} \\ e_z(x)e^{\gamma z} & W < X < A. \end{cases} \quad (12)$$

The tangential magnetic fields at the interface are discontinuous by the surface current densities, and assuming infinitesimally thin strip (can be considered as current sheet) the following boundary conditions can be written at $y=D$

$$H_{x_1}(x, D, z) - H_{x_2}(x, D, z) = \begin{cases} 0 & W < X < A \\ J_z(x)e^{\gamma z} & \text{on strip} \end{cases} \quad (13)$$

$$H_{z_1}(x, D, z) - H_{z_2}(x, D, z) = \begin{cases} 0 & W < X < A \\ J_x(x)e^{\gamma z} & \text{on strip.} \end{cases} \quad (14)$$

At the interface between region 1 and the upper wall of the waveguide ($y=H$) the tangential electric fields must be zero or explicitly writing

$$E_{x_1}(x, H, z) = 0 \quad (15)$$

$$E_{z_1}(x, H, z) = 0. \quad (16)$$

Substituting the field expressions of equations (1) through (6) into the boundary condition expressions of equations (7) through (16) yields the following equations:

$$\gamma \frac{\partial \phi_2^e(x,0)}{\partial x} - j\omega\mu_2 \frac{\partial \phi_2^h(x,0)}{\partial y} = 0 \quad (17)$$

$$Kc_2^2 \phi_2^e(x,0) = 0 \quad (18)$$

$$\gamma \frac{\partial \phi_1^e(X,D)}{\partial x} - j\omega\mu_1 \frac{\partial \phi_1^h(X,D)}{\partial y} = \gamma \frac{\partial \phi_2^e(X,D)}{\partial x} - j\omega\mu_2 \frac{\partial \phi_2^h(X,D)}{\partial y} \quad (19)$$

$$Kc_1^2 \phi_1^e(X,D) = Kc_2^2 \phi_2^e(X,D) \quad (20)$$

$$\gamma \frac{\partial \phi_1^e(X,D)}{\partial x} - j\omega\mu_1 \frac{\partial \phi_1^h(X,D)}{\partial y} = \begin{cases} 0 & \text{on strip} \\ e_x(x) & W < X < A \end{cases} \quad (21)$$

$$Kc_1^2 \phi_1^e(X,D) = \begin{cases} 0 & \text{on strip} \\ e_z(x) & W < X < A \end{cases} \quad (22)$$

$$\gamma \frac{\partial \phi_1^h(X,D)}{\partial x} + j\omega\epsilon_1 \frac{\partial \phi_1^e(X,D)}{\partial y} - \quad (23)$$

$$- \left(\gamma \frac{\partial \phi_2^h(X,D)}{\partial x} + j\omega\epsilon_2 \frac{\partial \phi_2^e(X,D)}{\partial y} \right) = \begin{cases} 0 & W < X < A \\ J_z(x) & \text{on strip} \end{cases}$$

$$Kc_1^2 \phi_1^h(X,D) - Kc_2^2 \phi_2^h(X,D) = \begin{cases} 0 & W < X < A \\ J_x(x) & \text{on strip} \end{cases} \quad (24)$$

$$\gamma \frac{\partial \phi_1^e(X,H)}{\partial x} - j\omega\mu_1 \frac{\partial \phi_1^h(X,H)}{\partial y} = 0 \quad (25)$$

$$Kc_1^2 \phi_1^e(X,H) = 0. \quad (26)$$

B. SPECTRAL DOMAIN TRANSFORM

The scalar potential functions ϕ_i^e and ϕ_i^h must satisfy Helmholtz's equations in the two spatial regions, thus

$$(\nabla_{xy}^2 + Kc_i^2) \phi_i^e(x,y) = 0 \quad (27)$$

$$(\nabla_{xy}^2 + Kc_i^2) \phi_i^h(x,y) = 0 \quad (28)$$

where $Kc_i^2 = \gamma^2 + K_i^2 = K_i^2 - \beta^2$ and ∇_{xy}^2 is a two-dimensional Laplacian operator.

As was suggested by Itoh and Mittra [Ref. 3] a Fourier transform was used in the α domain. The transform is defined by:

$$F_x[\phi_i(x,y)] = \phi_i(\alpha,y) = \int_{-\infty}^{\infty} \phi_i(x,y) e^{j\alpha x} dx \quad (29)$$

$i = 1,2.$

Since the structure is closed boundary, a finite Fourier transform must be used instead of the infinite Fourier transform. The finite Fourier transform is given by

$$F_x[\phi_i(x,y)] = \phi_i(\alpha n y) = \int_0^a \phi_i e^{j\alpha n x} dx \quad (30)$$

where $\alpha n = \frac{2 \cdot \pi \cdot n}{A}$

and

$$F_x\left[\frac{\partial \phi_i(x,y)}{\partial x}\right] = -j\alpha n F_x[\phi_i(x,y)]. \quad (31)$$

By using equations (30) and (31), a general transform of equations (27) and (28) is given by

$$F_x \left[\frac{\partial \phi_i^2(x,y)}{\partial x^2} \right] + F_x \left[\frac{\partial \phi_i^2(x,y)}{\partial y^2} \right] + Kc_i^2 F_x [\phi_i(x,y)] = 0 \quad (32)$$

Or explicitly writing:

$$\frac{\partial^2 \phi_i(\alpha_n y)}{\partial y^2} = \gamma_i^2 \phi_i(\alpha_n y) \quad (33)$$

where $\gamma_i^2 = \alpha_n^2 + \beta^2 - K_i^2$ $i = 1, 2$.

Equation (33) should be analyzed for both regions 1 and 2, and the solutions will be the transforms of the electric and magnetic scalar potentials for both regions.

For region 1,

$$\gamma_1^2 = \alpha_n^2 + \beta^2 - K_1^2 \quad (34)$$

Where $K_1 = \omega \sqrt{\epsilon_0 \mu_0} = \frac{2\pi}{\lambda_0}$ and $\beta = \frac{2\pi}{\lambda_T}$.

Substituting K_1 and β into equation (34) obtains,

$$\gamma_1^2 = \alpha_n^2 + \left(\frac{2\pi}{\lambda_0}\right)^2 \left[\left(\frac{\lambda_0}{\lambda_T}\right)^2 - 1 \right]. \quad (35)$$

λ' is the effective structure wavelength and is related to the free space wavelength λ_0 by

$$\frac{\lambda_0}{\sqrt{\epsilon_{r1}}} > \lambda' = \frac{\lambda_0}{\sqrt{\epsilon_{r_{eff}}}} \quad (36)$$

where $\epsilon_{r_{eff}}$ is the effective relative dielectric constant of the device.

Since $\epsilon_{r1} = 1$ in region 1, equation (36) can be rewritten as

$$\lambda_0 > \lambda' = \frac{\lambda_0}{\sqrt{\epsilon_{r_{eff}}}} \quad (37)$$

By using equation (37) together with equation (35) one can find that

$$\gamma_1^2 > \alpha_n^2 \quad (38)$$

Therefore γ_1 is always a real quantity.

For region 2:

$$\gamma_2^2 = \alpha_n^2 + \beta^2 - K_2^2 \quad (39)$$

$$\text{where } K_2 = \omega \sqrt{\mu_2 \epsilon_2} = \frac{2\pi}{\lambda_0} \sqrt{\mu_{r2} \epsilon_{r2}} \quad .$$

By substituting K_2 and β into equation (39) one can obtain

$$\gamma_2^2 = \alpha_n^2 - \left(\frac{2\pi}{\lambda_0}\right)^2 [\mu_{r2} \epsilon_{r2} = \left(\frac{\lambda_0}{\lambda'}\right)^2] \quad (40)$$

From equation (40) it is clear that γ_2 can be either a real or an imaginary quantity, depending on the value of αn .

γ_2 will be imaginary for

$$-\frac{2\pi}{\lambda_0} \sqrt{[\mu r_2 \epsilon r_2 - (\frac{\lambda_0}{\lambda})^2]} < \alpha n < \frac{2\pi}{\lambda_0} \sqrt{[\mu r_2 \epsilon r_2 - (\frac{\lambda_0}{\lambda})^2]} \quad (41)$$

and will be real for

$$-\infty < \alpha n < -\frac{2\pi}{\lambda_0} \sqrt{\mu r_2 \epsilon r_2 - (\frac{\lambda_0}{\lambda})^2}$$

$$\frac{2\pi}{\lambda_0} \sqrt{\mu r_2 \epsilon r_2 - (\frac{\lambda_0}{\lambda})^2} < \alpha n < \infty . \quad (42)$$

The last two equations should be carefully observed while solving equation (33).

For region 1 equation (33) can be written as

$$\frac{\partial^2 \phi_1(\alpha n, y)}{\partial y^2} = \gamma_1^2 \phi_1(\alpha n, y) \quad (43)$$

and the solution has the form of

$$\phi_1(\alpha n, y) = A(\alpha n) \cosh \gamma_1 \cdot y + B(\alpha n) \sinh \gamma_1 \cdot y \quad (44)$$

For region 2, two solutions do exist corresponding to the real and imaginary values of γ_2 .

For γ_2 real,

$$\phi_2(\alpha_n, y) = C(\alpha_n) \cosh \gamma_2 y + D(\alpha_n) \sinh \gamma_2 y \quad (45)$$

and for γ_2 imaginary

$$\phi_2(\alpha_n, y) = C(\alpha_n) \cos \gamma_2'' y + jD(\alpha_n) \sin \gamma_2'' y \quad (46)$$

where $\gamma_2 = j\gamma_2''$.

After knowing the solutions for $\phi_1(\alpha_n, y)$ and $\phi_2(\alpha_n, y)$, one can write the transforms of ϕ_1^e , ϕ_2^e , ϕ_1^h , ϕ_2^h in both regions as follows.

Region 1 $D \leq y \leq H$

$$\phi_1^e(\alpha_n, y) = A^e(\alpha_n) \cosh \gamma_1 (y-D) + B^e(\alpha_n) \sinh \gamma_1 (y-D) \quad (47)$$

$$\phi_1^h(\alpha_n, y) = A^h(\alpha_n) \cosh \gamma_1 (y-D) + B^h(\alpha_n) \sinh \gamma_1 (y-D) \quad (48)$$

Region 2 $0 \leq y \leq D$

$$\phi_2^e(\alpha_n, y) = \begin{cases} C_H^e(\alpha_n) \cosh \gamma_2 y + D_H^e(\alpha_n) \sinh \gamma_2 y, & (\gamma_2 \text{ real}) \\ C_T^e(\alpha_n) \cos \gamma_2'' y + jD_T^e(\alpha_n) \sin \gamma_2'' y, & (\gamma_2 \text{ imaginary}) \end{cases} \quad (49)$$

(50)

$$\phi_2^h(\alpha_n, y) = \begin{cases} C_H^h(\alpha_n) \cosh \gamma_2 y + D_H^h(\alpha_n) \sinh \gamma_2 y, & (\gamma_2 \text{ real}) \\ C_T^h(\alpha_n) \cos \gamma_2'' y + jD_T^h(\alpha_n) \sin \gamma_2'' y, & (\gamma_2 \text{ imaginary}) \end{cases} \quad (51)$$

(52)

Superscript (e) indicates the electric field case and (h) indicates the magnetic field case.

All coefficients that appear in equations (47) through (52) can be determined by the boundary condition expressions. The above can be done by taking the Fourier transform of equations (17) through (26), substituting the field expressions for both cases of γ_2 , real and imaginary, and finally solving for the coefficients.

The following equations are obtained:

Hyperbolic Case (γ_2 - real)

$$-j\alpha n \gamma C_H^e(\alpha n) - j\omega \mu_2 \gamma_2 D_H^h(\alpha n) = 0 \quad (53)$$

$$Kc_2^2 C_H^e(\alpha n) = 0 \quad (54)$$

$$Kc_1^2 A^e(\alpha n) = E_z(\alpha n) \quad (55)$$

$$-j\alpha n \gamma A^e(\alpha n) - j\omega \mu_1 \gamma_1 B_H^h(\alpha n) = E_x(\alpha n) \quad (56)$$

$$Kc_1^2 A^h(\alpha n) - Kc_2^2 [C_H^h(\alpha n) \cosh \gamma_2 D + D_H^h(\alpha n) \sinh \gamma_2 D] = J_x(\alpha n) \quad (57)$$

$$-j\alpha n\gamma A^h(\alpha n) + j\omega\epsilon_1\gamma_1 B^e(\alpha n) - \quad (58)$$

$$- \{-j\alpha n\gamma [C_H^h(\alpha n)\cosh\gamma_2 D + D_H^h(\alpha n)\sinh\gamma_2 D] + \\ + j\omega\epsilon_2 [\gamma_2 C_H^e(\alpha n)\sinh\gamma_2 D + \gamma_2 D_H^e(\alpha n)\cosh\gamma_2 D]\} = J_Z(\alpha n)$$

$$Kc_1^2 A^e(\alpha n) = Kc_2^2 [C_H^e(\alpha n)\cosh\gamma_2 D + D_H^e(\alpha n)\sinh\gamma_2 D] \quad (59)$$

$$- j\alpha n\gamma A^e(\alpha n) - j\omega\mu_1\gamma_1 B^h(\alpha) = \quad (60)$$

$$- j\alpha n\gamma [C_H^e(\alpha n)\cosh\gamma_2 D + D_H^e(\alpha n)\sinh\gamma_2 D] -$$

$$- j\omega\mu_2\gamma_2 [C_H^h(\alpha n)\sinh\gamma_2 D + D_H^h(\alpha n)\cosh\gamma_2 D]$$

$$- j\alpha n\gamma [A^e(\alpha n)\cosh\gamma_1(H-D) + B^e(\alpha n)\sinh\gamma_1(H-D)] - \quad (61)$$

$$- j\omega\mu_1\gamma_1 [A^h(\alpha n)\sinh\gamma_1(H-D) + B^h(\alpha n)\cosh\gamma_1(H-D)] = 0$$

$$Kc_1^2 [A^e(\alpha n)\cosh\gamma_1(H-D) + B^e(\alpha n)\sinh\gamma_1(H-D)] = 0. \quad (62)$$

The coefficients for the hyperbolic case are obtained as follows:

$$C_H^e(\alpha n) = 0 \quad (63)$$

$$A^e(\alpha n) = \frac{E_Z(\alpha n)}{Kc_1^2} \quad (64)$$

$$D_H^h(\alpha n) = 0 \quad (65)$$

$$B^h(\alpha n) = -\frac{\alpha n\gamma}{\omega\mu_1\gamma_1 Kc_1^2} E_Z(\alpha n) + j\frac{1}{\omega\mu_1\gamma_1} E_X(\alpha n) \quad (66)$$

$$D_H^e(\alpha n) = \frac{1}{Kc_2^2 \sinh \gamma_2 D} E_Z(\alpha n) \quad (67)$$

$$C_H^h(\alpha n) = - \frac{\alpha n \gamma}{Kc_2^2 \omega \mu_2 \gamma_2 \sinh \gamma_2 D} E_Z(\alpha n) + j \frac{1}{\omega \mu_2 \gamma_2 \sinh \gamma_2 D} E_X(\alpha n) \quad (68)$$

$$B^e(\alpha n) = - \frac{\text{ctgh} \gamma_1 (H-D)}{Kc_1^2} E_Z(\alpha n) \quad (69)$$

$$A^h(\alpha n) = \frac{\alpha n \cdot \gamma \cdot \text{ctgh} \gamma_1 (H-D)}{\omega \mu_1 \gamma_1 Kc_1^2} E_Z(\alpha n) - j \frac{\text{ctgh} \gamma_1 (H-D)}{\omega \mu_1 \gamma_1} E_X(\alpha n) \quad (70)$$

When substituting equation (63) through (70) into equations (57) and (58) one can form two sets of equations

$$F_1^H(\alpha n, \beta) E_X(\alpha n) + F_2^H(\alpha n, \beta) E_Z(\alpha n) = J_X(\alpha n) \quad (71)$$

$$F_3^H(\alpha n, \beta) E_X(\alpha n) + F_4^H(\alpha n, \beta) E_Z(\alpha n) = J_Z(\alpha n) \quad (72)$$

or in matrix form

$$\begin{bmatrix} F_1^H(\alpha n, \beta) & F_2^H(\alpha n, \beta) \\ F_3^H(\alpha n, \beta) & F_4^H(\alpha n, \beta) \end{bmatrix} \begin{bmatrix} E_X(\alpha n) \\ E_Z(\alpha n) \end{bmatrix} = \begin{bmatrix} J_X(\alpha n) \\ J_Z(\alpha n) \end{bmatrix} \quad (73)$$

where $\gamma = j\beta$.

The elements of the matrix $[F^H]$ are given as follows:

$$F_1^H(\alpha n, \beta) = -j \left[\frac{Kc_1^2 \operatorname{ctgh} \gamma_1 (H-D)}{\omega \mu_1 \gamma_1} + \frac{Kc_2^2 \operatorname{ctgh} \gamma_2 D}{\omega \mu_2 \gamma_2} \right] \quad (74)$$

$$F_2^H(\alpha n, \beta) = j \left[\frac{\alpha n \beta \operatorname{ctgh} \gamma_1 (H-D)}{\omega \mu_1 \gamma_1} + \frac{\alpha n \beta \operatorname{ctgh} \gamma_2 D}{\omega \mu_2 \gamma_2} \right] \quad (75)$$

$$F_3^H(\alpha n, \beta) = -F_2^H(\alpha n, \beta) \quad (76)$$

$$F_4^H(\alpha n, \beta) = j \left[\frac{(\alpha n \beta)^2 \operatorname{ctgh} \gamma_1 (H-D)}{\omega \mu_1 \gamma_1 Kc_1^2} - \frac{\omega \epsilon_1 \gamma_1 \operatorname{ctgh} \gamma_1 (H-D)}{Kc_1^2} - \right. \\ \left. - \frac{\omega \epsilon_2 \gamma_2 \operatorname{ctgh} \gamma_2 D}{Kc_2^2} + \frac{(\alpha n \beta)^2 \operatorname{ctgh} \gamma_2 D}{Kc_2^2 \omega \mu_2 \gamma_2} \right]. \quad (77)$$

The same method can be applied to the trigonometric case (γ_2 imaginary) and the following equations are obtained:

$$C_T^e(\alpha n) = 0 \quad (78)$$

$$D_T^h(\alpha n) = 0 \quad (79)$$

$$D_T^e(\alpha n) = -j \frac{1}{Kc_2^2 \sin \gamma_2 "D} E_Z(\alpha n) \quad (80)$$

$$C_T^h(\alpha n) = \frac{\alpha n \gamma}{Kc_2^2 \omega \mu_2 \gamma_2 " \sin \gamma_2 "D} E_Z(\alpha n) - j \frac{1}{\omega \mu_2 \gamma_2 " \sin \gamma_2 "D} E_X(\alpha n) \quad (81)$$

$$Kc_1^2 A^h(\alpha n) - Kc_2^2 [C_T^h(\alpha n) \cos \gamma_2 "D + j D_T^h(\alpha n) \sin \gamma_2 "D] = \\ = J_X(\alpha n) \quad (82)$$

$$\begin{aligned}
& -j\alpha n \gamma A^h(\alpha n) + j\omega \epsilon_1 \gamma_1 B^e(\alpha n) - j\alpha n \gamma C_T^h(\alpha n) \cos \gamma_2 "D + \\
& + \omega \epsilon_2 \gamma_2 "D T^e(\alpha n) \cos \gamma_2 "D = J_z(\alpha n) .
\end{aligned} \tag{83}$$

When substituting equations (69), (70) and (78) through (81) into equations (82) and (83) one can obtain the matrix form

$$\begin{bmatrix} F_1^T(\alpha n, \beta) & F_2^T(\alpha n, \beta) \\ F_3^T(\alpha n, \beta) & F_4^T(\alpha n, \beta) \end{bmatrix} \begin{bmatrix} E_x(\alpha n) \\ E_z(\alpha n) \end{bmatrix} = \begin{bmatrix} J_x(\alpha n) \\ J_z(\alpha n) \end{bmatrix} \tag{84}$$

where again $\gamma = j\beta$

and the elements of the matrix $[F^T]$ are given as follows:

$$F_1^T(\alpha n, \beta) = -j \left[\frac{Kc_1^2 \text{ctgh} \gamma_1 (H-D)}{\omega \mu_1 \gamma_1} - \frac{Kc_2^2 \text{ctg} \gamma_2 "D}{\omega \mu_2 \gamma_2 "D} \right] \tag{85}$$

$$F_2^T(\alpha n, \beta) = j \left[\frac{\alpha n \beta \text{ctgh} \gamma_1 (H-D)}{\omega \mu_1 \gamma_1} - \frac{\alpha n \beta \text{ctg} \gamma_2 "D}{\omega \mu_2 \gamma_2 "D} \right] \tag{86}$$

$$F_3^T(\alpha n, \beta) = -F_2^T(\alpha n, \beta) \tag{87}$$

$$\begin{aligned}
F_4^T(\alpha n, \beta) = j \left[\frac{(\alpha n \beta)^2 \text{ctgh} \gamma_1 (H-D)}{\omega \mu_1 \gamma_1 Kc_1^2} - \frac{\omega \epsilon_1 \gamma_1 \text{ctgh} \gamma_1 (H-D)}{Kc_1^2} - \right. \\
\left. - \frac{(\alpha n \beta)^2 \text{ctg} \gamma_2 "D}{Kc_2^2 \omega \mu_2 \gamma_2 "D} - \frac{\omega \epsilon_2 \gamma_2 "D \text{ctg} \gamma_2 "D}{Kc_2^2} \right] .
\end{aligned} \tag{88}$$

Expressions (73) and (84) can be written in a general form as

$$\begin{bmatrix} F_1^{H,T}(\alpha, \beta) & F_2^{H,T}(\alpha, \beta) \\ F_3^{H,T}(\alpha, \beta) & F_4^{H,T}(\alpha, \beta) \end{bmatrix} \begin{bmatrix} E_X(\alpha) \\ E_Z(\alpha) \end{bmatrix} = \begin{bmatrix} J_X(\alpha) \\ J_Z(\alpha) \end{bmatrix} \quad (89)$$

from which solutions to $E_X(\alpha)$ and $E_Z(\alpha)$ in terms of $J_X(\alpha)$ and $J_Z(\alpha)$ can be obtained as follows:

$$E_X(\alpha) = \frac{J_X(\alpha)F_4^{H,T}(\alpha, \beta) - J_Z(\alpha)F_2^{H,T}(\alpha, \beta)}{F_1^{H,T}(\alpha, \beta) \cdot F_4^{H,T}(\alpha, \beta) - F_2^{H,T}(\alpha, \beta) \cdot F_3^{H,T}(\alpha, \beta)} \quad (90)$$

$$E_Z(\alpha) = \frac{-J_X(\alpha)F_3^{H,T}(\alpha, \beta) + J_Z(\alpha) \cdot F_1^{H,T}(\alpha, \beta)}{F_1^{H,T}(\alpha, \beta) F_4^{H,T}(\alpha, \beta) - F_2^{H,T}(\alpha, \beta) \cdot F_3^{H,T}(\alpha, \beta)} \quad (91)$$

Define the following terms

$$DN = F_1^{H,T}(\alpha, \beta) F_4^{H,T}(\alpha, \beta) - F_2^{H,T}(\alpha, \beta) F_3^{H,T}(\alpha, \beta) \quad (92)$$

$$M_1^{H,T}(\alpha, \beta) = \frac{F_4^{H,T}(\alpha, \beta)}{DN} \quad (93)$$

$$M_2^{H,T}(\alpha, \beta) = -\frac{F_2^{H,T}(\alpha, \beta)}{DN} \quad (94)$$

$$M_3^{H,T}(\alpha, \beta) = -\frac{F_3^{H,T}(\alpha, \beta)}{DN} = -M_2^{H,T}(\alpha, \beta) \quad (95)$$

$$M_4^{H,T}(\alpha, \beta) = \frac{F_1^{H,T}(\alpha, \beta)}{DN} \quad (96)$$

which lead to the final expressions

$$E_x(\alpha n) = M_1^{H,T}(\alpha n, \beta) J_x(\alpha n) + M_2^{H,T}(\alpha n, \beta) J_z(\alpha n) \quad (97)$$

$$E_z(\alpha n) = M_3^{H,T}(\alpha n, \beta) J_x(\alpha n) + M_4^{H,T}(\alpha n, \beta) J_z(\alpha n) . \quad (98)$$

C. DETERMINENTAL EQUATION

Nothing seems to be gained so far since neither the electric field and the current density components nor their transforms are known. In order to simplify equation (97) and (98), the method of moments [Ref. 4] is applied in the spectral domain. Define a scalar product over the domain $-\infty < \alpha n < \infty$ according to reference 6 as

$$\langle a(\alpha n), b(\alpha n) \rangle = \sum_{n=-\infty}^{n=\infty} a(\alpha n) \cdot b^*(\alpha n). \quad (99)$$

Thus when applying this concept to equation (95) and (96) and choosing $a(\alpha n) = E_x(\alpha n)$ or $J_z(\alpha n)$ and $b(\alpha n) = J_x(\alpha n)$ or $J_z(\alpha n)$ respectively, one can obtain

$$\langle M_1^{H,T}(\alpha n, \beta) J_x(\alpha n), J_x(\alpha n) \rangle + \langle M_2^{H,T}(\alpha n, \beta) J_z(\alpha n), J_x(\alpha n) \rangle = 0 \quad (100)$$

$$\langle M_3^{H,T}(\alpha n, \beta) J_x(\alpha n), J_z(\alpha n) \rangle + \langle M_4^{H,T}(\alpha n, \beta) J_z(\alpha n), J_z(\alpha n) \rangle = 0. \quad (101)$$

By using Parseval's theorem it can easily be shown that the right hand side of the above two equations is equal to zero, due to the orthogonality of $E_z(\alpha n)$ and $J_z(\alpha n)$, and $E_x(\alpha n)$ and $J_x(\alpha n)$.

In general, one can expand each current density component in a set of basis functions such as:

$$J_z(x) = \sum_{k=1}^{\infty} a_{1k} f'_{zk}(x) \quad (102)$$

$$J_x(x) = \sum_{k=1}^{\infty} a_{2k} g'_{zk}(x) \quad (103)$$

In the following analysis, one term approximation is used since it was found to be less complicated, without much degradation in the accuracy of the final results.

So with

$$J_z(\alpha n) = F\{a_1 \cdot f'_z(x)\} = a_1 f_z(\alpha n) \quad (104)$$

and

$$J_x(\alpha n) = F\{a_2 \cdot g'_x(x)\} = a_2 \cdot g_x(\alpha n) \quad (105)$$

equations (100) and (101) become

$$a_2 \sum_{n=-\infty}^{\infty} M_1^{H,T}(\alpha n, \beta) |g_x(\alpha n)|^2 + a_1 \sum_{n=-\infty}^{\infty} M_2^{H,T}(\alpha n, \beta) \quad (106)$$

$$f_z(\alpha n) g_x^*(\alpha n) = 0$$

$$a_2 \sum_{n=-\infty}^{\infty} M_3^{H,T}(\alpha n, \beta) g_x(\alpha n) f_z^*(\alpha n) + a_1 \sum_{n=-\infty}^{\infty} M_4^{H,T}(\alpha n, \beta) \cdot |f_z(\alpha n)|^2 = 0. \quad (107)$$

From the geometry of the device (Fig. 3) and the location of the coordinate system it is clear that all choices of current density distributions, $J_z(x)$ and $J_x(x)$, are neither even nor odd functions.

Each current density distribution can be expressed as a linear function of even and odd functions as follows:

$$J_z(x) = a_1 [f'_{ze}(x) + f'_{zo}(x)] \quad (108)$$

$$J_x(x) = a_2 [g'_{xe}(x) + g'_{xo}(x)] \quad (109)$$

When taking the Fourier transform of equations (108) and (109) then according to reference 7, the following transforms are obtained

$$J_z(\alpha n) = a_1 [f_{ze}(\alpha n) + j f_{zo}(\alpha n)] = a_1 f_z(\alpha n) \quad (110)$$

$$J_x(\alpha n) = a_2 [g_{xe}(\alpha n) + j g_{xo}(\alpha n)] = a_2 g_x(\alpha n). \quad (111)$$

In order to solve equations (106) and (107) for the non-trivial solution, the determinant of the coefficient matrix should be set to zero for all sets of physical parameters, at each frequency of operation. The above can be

achieved by finding the appropriate β that satisfies this requirement. From that β the dispersion characteristics of the device can be calculated.

The determinantal equation has the form of

$$\left[\sum_{n=-\infty}^{\infty} M_1^{H,T}(\alpha n, \beta) |g_x(\alpha n)|^2 \right] \cdot \left[\sum_{n=-\infty}^{\infty} M_4^{H,T}(\alpha n, \beta) |f_z(\alpha n)|^2 \right] - \left[\sum_{n=-\infty}^{\infty} M_2^{H,T}(\alpha n, \beta) \cdot f_z(\alpha n) g_x^*(\alpha n) \right] \cdot \left[\sum_{n=-\infty}^{\infty} M_3^{H,T}(\alpha n, \beta) g_x(\alpha n) f_z^*(\alpha n) \right] = 0 \quad (112)$$

By investigating equations (93) through (96) one may observe that $M_1(\alpha n, \beta)$ and $M_4(\alpha n, \beta)$ are even functions, while $M_2(\alpha n, \beta)$ and $M_3(\alpha n, \beta)$ are odd functions.

Using this information together with equations (110) and (111) leads to the final expression of the determinantal equation

$$\left[\sum_{n=-\infty}^{\infty} M_1^{H,T}(\alpha n, \beta) |g_x(\alpha n)|^2 \right] \cdot \left[\sum_{n=-\infty}^{\infty} M_4^{H,T}(\alpha n, \beta) |f_z(\alpha n)|^2 \right] + \left[\sum_{n=-\infty}^{\infty} M_2^{H,T}(\alpha n, \beta) \cdot B(\alpha n) \right]^2 = 0 \quad (113)$$

where

$$B(\alpha n) = -f_{ze}(\alpha n) \cdot g_{xo}(\alpha n) + f_{zo}(\alpha n) \cdot g_{xe}(\alpha n). \quad (114)$$

In addition to the requirement that the determinant of the coefficients matrix should be set to zero, one can see from equations (106), (113) and (114) that the ratio of the two coefficients has the form of

$$\frac{a_1}{a_2} = j \left[\frac{\sum_{n=-\infty}^{\infty} M_1^{H,T}(\alpha n, \beta) |g_x(\alpha n)|^2}{\sum_{n=-\infty}^{\infty} M_2^{H,T}(\alpha n, \beta) B(\alpha n)} \right] \quad (115)$$

Since the expression in the brackets is a real quantity, it is well understood that there is a 90° phase difference (in time) between the two current density components.

D. CURRENT DENSITY COMPONENTS

After the determinantal equation was simplified as shown in equation (113), the two current density components $J_z(x)$ and $J_x(x)$ were approximated, thus that the equation could have been solved. Various one term approximations were investigated and the set of components that was chosen to be substituted in the determinantal equation was the one found as the best approximation of both current distribution components.

The approximated current density component in the z-direction has the form

$$J_z(x) = \begin{cases} a_1 e^{20 \frac{x}{W}} & \text{on the strip} \\ 0 & \text{elsewhere} \end{cases} \quad (116)$$

and in the x-direction

$$J_x(x) = \begin{cases} a_2 \cos \frac{\pi x}{2W} & \text{on the strip} \\ 0 & \text{elsewhere} \end{cases} \quad (117)$$

The two current density components are shown in Figure 4.

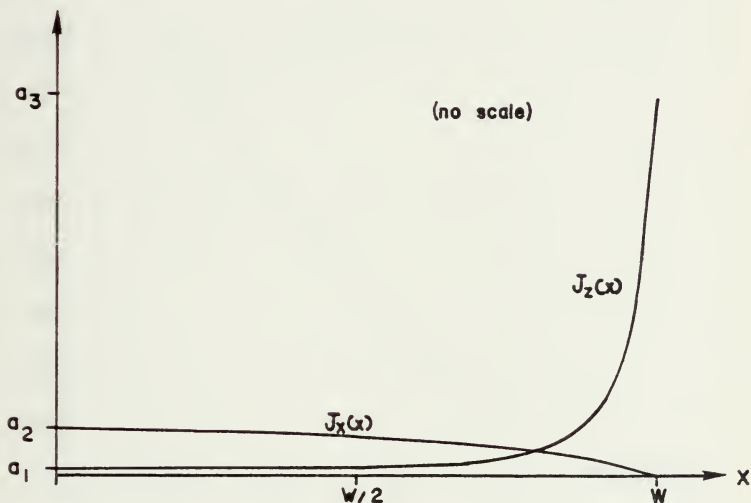


Figure 4. Longitudinal and Transverse Current Density Components.

It is clear that the ratio $a_3/a_1 = e^{20} = 4.85 \cdot 10^8$ indicates that most of the current that flows in the z-direction is concentrated at the right edge of the strip [Fig. 3]. On the other hand the choice of $J_x(x)$ indicates that there is no current in the x-direction at the right-edge of the strip.

Computer output indicated a frequency dependent of the ratio a_3/a_2 as shown in Figure 5. This curve was plotted for $D = 0.125''$ $w = 0.45''$ $\epsilon_r = 16$ and $a_1 = 10^{-10}$.

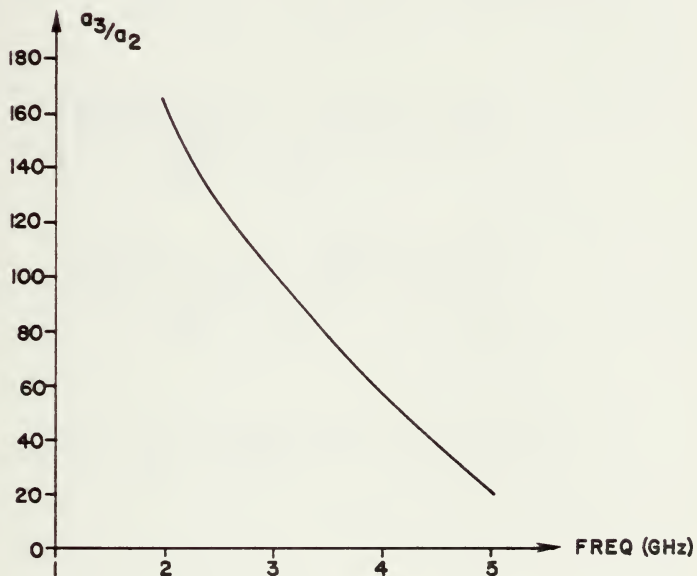


Figure 5. Ratio of the Maximum Current Density Components

From Figure 5 one may learn that the transverse current component on the strip increases relative to the longitudinal component, as the frequency increases.

The Fourier transforms of the current density components are given as:

$$J_z(\alpha n) = \int_0^W a_1 e^{20 \frac{x}{W}} e^{j\alpha n x} dx = a_1 \cdot f_z(\alpha n) = \quad (118)$$

$$= a_1 \left[\frac{\frac{20}{W}(e^{20} \cos \alpha n W - 1) + e^{20} \cdot \alpha n \cdot \sin \alpha n W}{\left(\frac{20}{W}\right)^2 + (\alpha n)^2} + \right. \\ \left. + j \frac{-\alpha n (e^{20} \cos \alpha n W - 1) + \frac{20}{W} e^{20} \sin \alpha n W}{\left(\frac{20}{W}\right)^2 + (\alpha n)^2} \right]$$

$$J_x(\alpha n) = \int_0^W a_2 \cos \frac{\pi x}{2W} e^{j\alpha n x} dx = a_2 \cdot g_x(\alpha n) = \quad (119)$$

$$= a_2 \left[\frac{\frac{\pi}{2W} \cos \alpha n W}{\left(\frac{\pi}{2W}\right)^2 - (\alpha n)^2} + j \frac{\frac{\pi}{2W} \sin \alpha n W + \alpha n}{\left(\frac{\pi}{2W}\right)^2 - (\alpha n)^2} \right]$$

where the even and odd components of each transform can be identified by referring to equations (110) and (111).

After substituting equations (118) and (119) into equation (113), the determinantal equation was programmed into Fortran language and the root β that set the determinantal

equation equal to zero, was found by an iteration method on a digital computer. From the value of β , λ'/λ could easily be calculated.

Figure 6 shows:

1. Computed and measured λ'/λ vs. frequency for $D = 0.125"$, $W = 0.45"$, $\epsilon_r = 16$.
2. Computed λ'/λ vs. frequency for $D = 0.025"$, $w = 0.45"$, $\epsilon_r = 16$.

Both curves are plotted for $A = 0.9"$, $H = 0.4"$.

It can be seen that there is a good agreement between experimental and computed wavelength ratio. The highest deviation is on the order of 10 percent which can be attributed largely to the experimental apparatus.

One can learn that the wavelength's ratio is directly proportional to the dielectric substrate width, which implies that the fields are more confined in the dielectric substrate as its width decreases.

E. AVERAGE POWER FLOW

For later discussion of the characteristics of the device built on ferrite substrate, a perturbation technique is used. One of the entries to the perturbation expression is the average power flow in the device built on a dielectric substrate.

A general expression for the time average power flow in the direction of propagation is given by

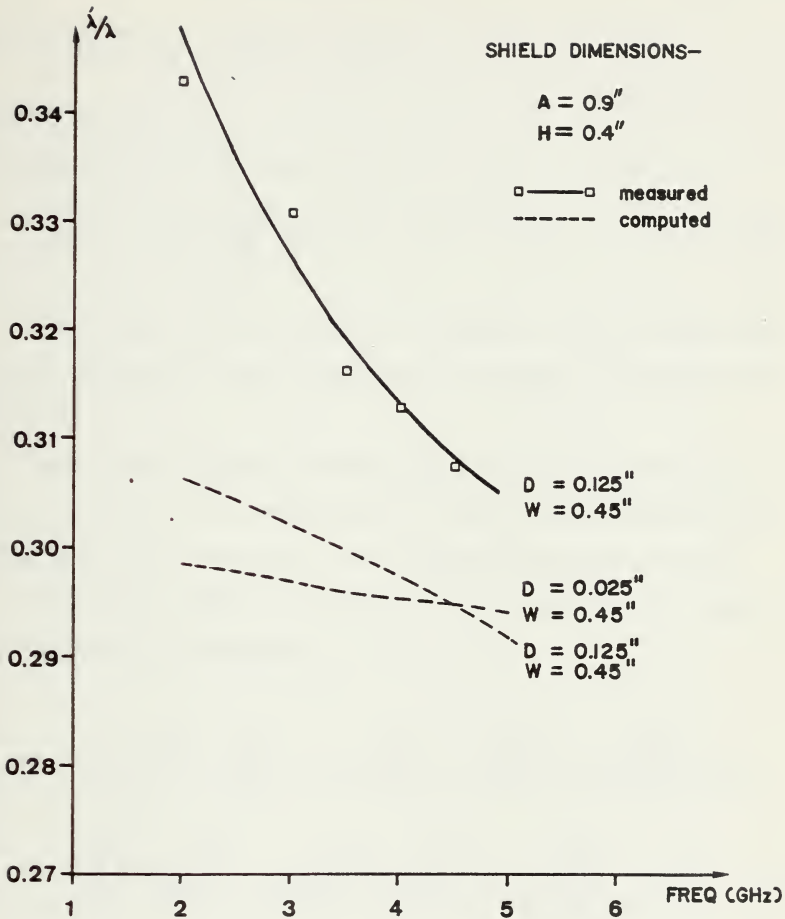


Figure 6. Computed and Measured Dispersion Characteristics for D = 0.025" W = 0.45" and D = 0.125" W = 0.45" with $\epsilon_r = 16$.

$$P_{ave} = \frac{1}{2} \operatorname{Re} \iint_S (\vec{E} \times \vec{H}^*) \cdot \hat{a}_z \, da \quad (120)$$

$$\text{Since } (\vec{E} \times \vec{H}^*) \cdot \hat{a}_z = E_x H_y^* - E_y H_x^*$$

and $da = dx \, dy$

then equation (120) can be rewritten as

$$P_{ave} = -\frac{1}{2} \operatorname{Re} \iint_S (E_x H_y^* - E_y H_x^*) \, dx \, dy \quad (121)$$

The minus sign was added in equation (121) to make the result positive (recall propagation in the $-z$ direction was assumed).

Both the electric and the magnetic fields are known in terms of the scalar potentials ϕ^e and ϕ^h thus substituting equations (3) through (6) into equation (121) and using $\gamma = j\beta$ for the waves traveling in the $-z$ direction, leads to the following expression

$$P_{i \, ave} = -\frac{1}{2} \operatorname{Re} \left\{ \iint_S \left(j\beta \frac{\partial \phi_i^e}{\partial x} - j\omega \mu_i \frac{\partial \phi_i^h}{\partial y} \right) \left(-j\beta \frac{\partial \phi_i^h}{\partial y} + j\omega \epsilon_i \frac{\partial \phi_i^e}{\partial x} \right) dx dy + \right. \\ \left. + \iint_S \left(j\beta \frac{\partial \phi_i^e}{\partial y} + j\omega \mu_i \frac{\partial \phi_i^h}{\partial x} \right) \left(j\beta \frac{\partial \phi_i^h}{\partial x} + j\omega \epsilon_i \frac{\partial \phi_i^e}{\partial y} \right) dx dy \right\} \quad (122)$$

$i=1,2$

Subscript i denotes the spatial regions, air and dielectric substrate respectively, for which equation (122) must be evaluated.

The total average power flow in the device is the sum of the spatial power components that flow both in the air and in the dielectric substrate as shown in the following equation

$$P_{ave_{TOT}} = P_{1ave} + P_{2ave} \quad (123)$$

Applying Parseval's theorem to equation (122) obtains

$$P_{iave} = -\frac{1}{2A} \operatorname{Re} \sum_{n=-\infty}^{\infty} \int \left\{ -\alpha n^2 \omega \beta \epsilon_i |\phi_i^e(\alpha n, y)|^2 - \right. \quad (124)$$

$$- \alpha n^2 \omega \beta \mu_i |\phi_i^h(\alpha n, \beta)|^2 - \omega \beta \mu_i \left| \frac{\partial \phi_i^h(\alpha n, y)}{\partial y} \right|^2 -$$

$$- \omega \beta \epsilon_i \left| \frac{\partial \phi_i^e(\alpha n, y)}{\partial y} \right|^2 - j \alpha n \beta^2 \left[\phi_i^e(\alpha n, y) \frac{\partial \phi_i^{h*}(\alpha n, y)}{\partial y} + \right.$$

$$+ \phi_i^{h*} \frac{\partial \phi_i^e(\alpha n, y)}{\partial y} \left. \right] + j \alpha n K_i^2 \left[\phi_i^{e*} \frac{\partial \phi_i^h(\alpha n, y)}{\partial y} + \right.$$

$$\left. + \phi_i^{h*} \frac{\partial \phi_i^{e*}(\alpha n, y)}{\partial y} \right] \Bigg\} dy$$

The limits of integration depend on each region and are \int_0^H for region 1 and \int_0^D for region 2.

After obtaining the general expression for average power flow, one can apply it for both regions.

Recall equations (47), (48), (64), (66), (69) and (70) and have the first two modified, the following equations can be obtained

$$\phi_1^e(\alpha n, y) = A^{\bar{e}}(\alpha n) \sin h \gamma_1 (y-H) \quad (125)$$

$$\phi_1^h(\alpha n, y) = A^{\bar{h}}(\alpha n) \cos h \gamma_1 (y-H) \quad (126)$$

where

$$A^{\bar{e}}(\alpha n) = \frac{E_z(\alpha n)}{Kc_1^2 \sin h \gamma_1 (D-H)} \quad (127)$$

$$A^{\bar{h}}(\alpha n) = -j \left[\frac{\alpha n \beta E_z(\alpha n)}{Kc_1^2} - E_x(\alpha n) \right] \frac{1}{\omega \mu_1 \gamma_1 \sin h \gamma_1 (D-H)} \quad (128)$$

After using the modified expressions for $\phi_1^e(\alpha n, y)$ and $\phi_1^h(\alpha n, y)$ in region 1, and integrating with respect to y , one can obtain

$$P_{1 \text{ ave}} = \frac{1}{4A} \operatorname{Re} \sum_{n=-\infty}^{\infty} \left\{ \omega \beta \left[\frac{\sin h 2\gamma_1 (H-D)}{2\gamma_1} - (H-D) \right] \left[\alpha n^2 \epsilon_1 |A^{\bar{e}}(\alpha n)|^2 + \gamma_1^2 \mu_1 |A^{\bar{h}}(\alpha n)|^2 \right] + \omega \beta \left[\frac{\sinh 2\gamma_1 (H-D)}{2\gamma_1} + (H-D) \right] \left[\alpha n^2 \mu_1 |A^{\bar{h}}(\alpha n)|^2 + \gamma_1^2 \epsilon_1 |A^{\bar{e}}(\alpha n)|^2 \right] + j \alpha n \left[\beta^2 A^{\bar{e}}(\alpha n) A^{\bar{h}*}(\alpha n) - K_1^2 A^{\bar{e}*}(\alpha n) A^{\bar{h}}(\alpha n) \right] \sinh 2\gamma_1 (H-D) \right\} \quad (129)$$

In region 2, there are two expressions depending upon whether γ_2 is a real or imaginary quantity. As in region 1, the integration with respect to y can be done analytically, and the following equations are obtained.

For γ_2 real,

$$\begin{aligned}
 P_{2\text{ave}_H} = \frac{1}{4A} \operatorname{Re} \sum_{n=-\infty}^{\infty} \left\{ \omega\beta \left[\alpha n^2 \epsilon_2 |D_H^e(\alpha n)|^2 + \right. \right. & \quad (130) \\
 + \gamma_2^2 \mu_2 |C_H^h(\alpha n)|^2 \left. \right] \left[\frac{\sinh 2\gamma_2 D}{2\gamma_2} - D \right] + \omega\beta \left[\alpha n^2 \mu_2 |C_H^h(\alpha n)|^2 + \right. & \\
 + \gamma_2^2 \epsilon_2 |D_H^e(\alpha n)|^2 \left. \right] \left[\frac{\sinh 2\gamma_2 D}{2\gamma_2} + D \right] + j\alpha n \left[\beta^2 D_H^e(\alpha n) C_H^{h*}(\alpha n) - \right. & \\
 \left. - K_2^2 D_H^{e*}(\alpha n) C_H^h(\alpha n) \right] \sinh 2\gamma_2 D \left. \right\} &
 \end{aligned}$$

and for γ_2 imaginary, ($\gamma_2 = j\gamma_2''$)

$$\begin{aligned}
 P_{2\text{ave}_T} = \frac{1}{4A} \operatorname{Re} \sum_{n=-\infty}^{\infty} \left\{ \omega\beta \left[\alpha n^2 \epsilon_2 |D_T^e|^2 + \gamma_2''^2 \mu_2 |C_T^h|^2 \right] \cdot \right. & \quad (131) \\
 \cdot \left[D - \frac{\sin 2\gamma_2'' D}{2\gamma_2''} \right] + \omega\beta \left[\alpha n^2 \mu_2 |C_T^h|^2 + \right. & \\
 + \gamma_2''^2 \epsilon_2 |D_T^e|^2 \left. \right] \left[D + \frac{\sin 2\gamma_2'' D}{2\gamma_2''} \right] + & \\
 + \alpha n \left[\beta^2 D_T^e C_T^{h*} + K_2^2 C_T^h D_T^{e*} \right] \sin 2\gamma_2'' D \left. \right\} &
 \end{aligned}$$

$D_H^e(\alpha n)$, $C_H^h(\alpha n)$, $D_T^e(\alpha n)$ and $C_T^h(\alpha n)$ are given in equation (67), (68), (80) and (81) respectively

The total power in region 2 becomes

$$P_{2ave} = P_{2ave_H} + P_{2ave_T} \quad (132)$$

Detailed development of equations (129) through (131) is given in appendix A.

Curves of α -domain power distributions for regions 1 and 2 are shown in Figures 7 and 8 respectively. The ratio of the power carried in each region to the total power carried in the device for various parameters, is plotted as a function of frequency in Figures 9 and 10.

Several facts can be studied from the graphs.

- (a) The amount of power carried in each region is frequency dependent.
- (b) As frequency increases relatively more power is carried through region 2, the dielectric substrate.
- (c) Relatively more power is carried through region 1 as the permittivity is lowered.
- (d) In the low frequency region, more power is carried through region 1 as the substrate thickness increases. At high frequencies the power carried in region 1 approaches the same value, for all values of substrate thickness.
- (e) As strip width increases more power is carried through region 2, the dielectric substrate,

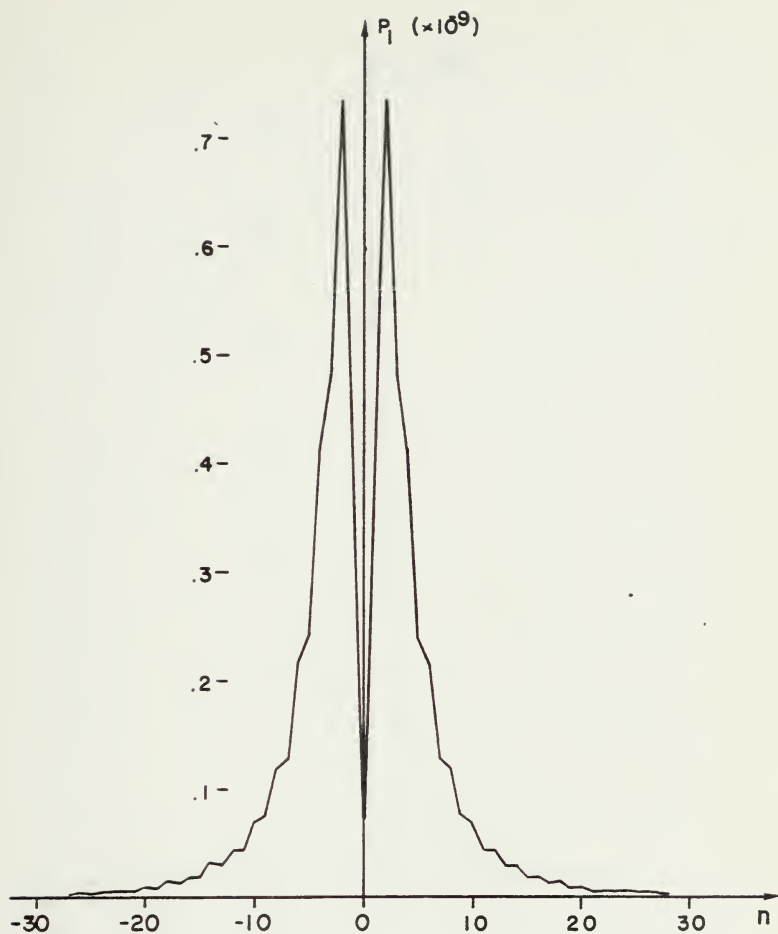


Figure 7. Average Power Distribution in Region 1 Vs. n (αn) for $f = 4\text{GHz}$, $D = 0.125''$, $W = 0.45''$, $\epsilon_r = 16$.

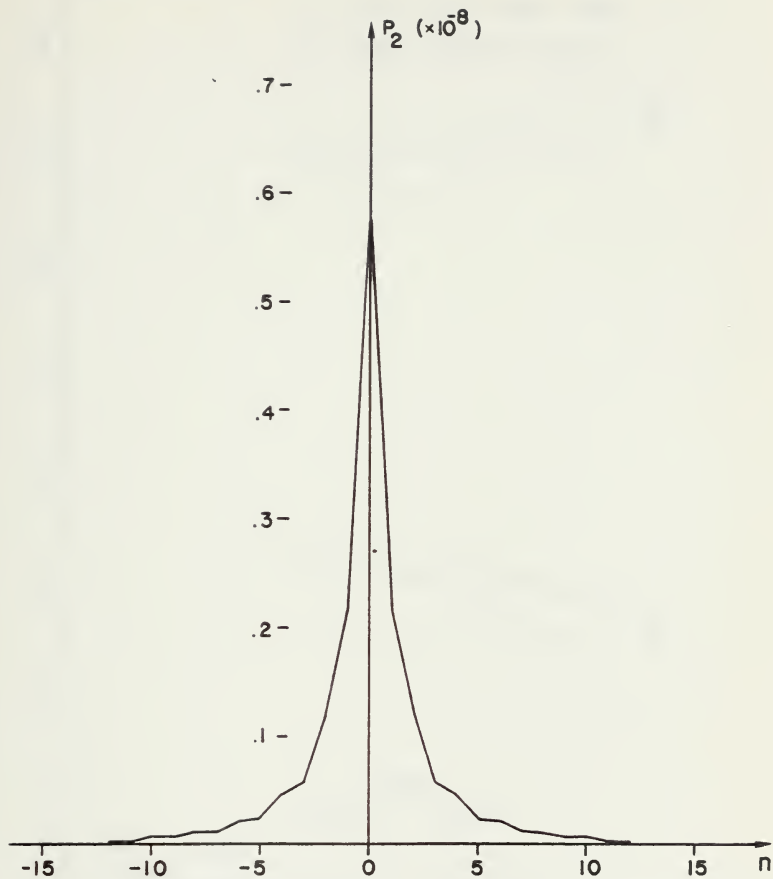


Figure 8. Average Power Distribution in Region 2 Vs. n (αn) for $f = 4\text{GHz}$, $D = 0.125''$, $W = 0.45''$, $\epsilon_r = 16$.

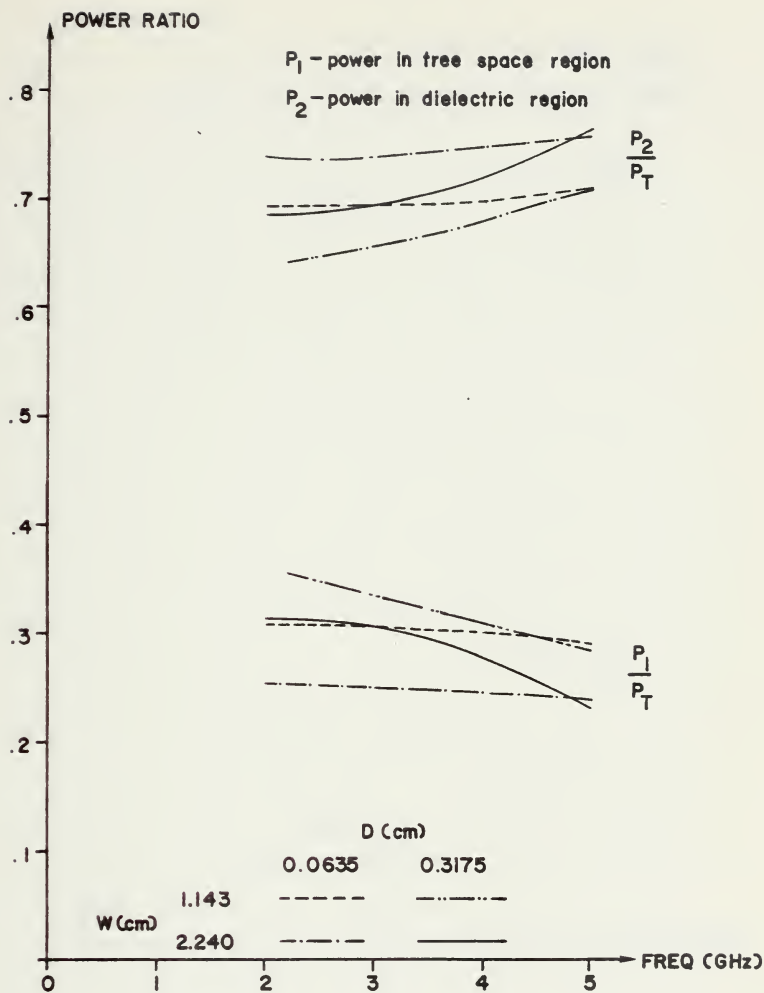


Figure 9. Average Power Ratio in Regions 1 and 2 Vs. Frequency for $\epsilon_r = 9$.

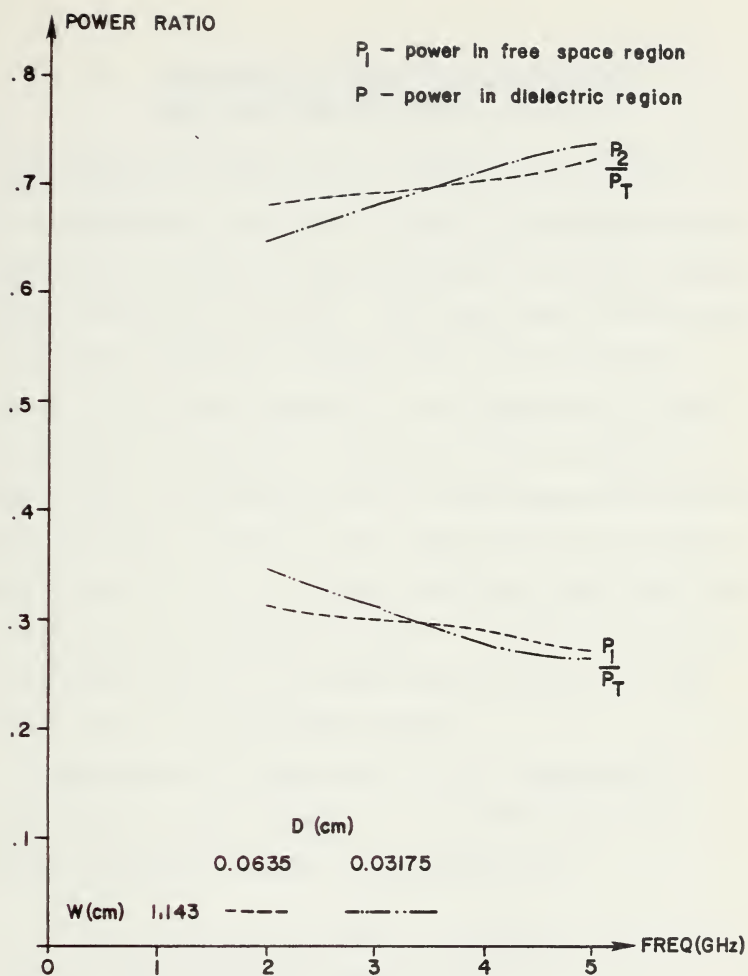


Figure 10. Average Power Ratio in Regions 1 and 2 Vs. Frequency for $\epsilon_r = 16$.

III. PERTURBATION ANALYSIS OF EDGE-GUIDED MODE ISOLATOR ON FERRITE SUBSTRATE

A. PERTURBATION EXPRESSION FOR PROPAGATION CONSTANT

Perturbational analysis is used to determine solutions for perturbed problems slightly changed from other problems to which solutions are known. The study that was done up to this point obtained a solution for the propagation constant of an electro-magnetic wave traveling in a structure as shown in Figure 3. The goal of this study as was stated in the introduction, was to investigate the characteristics of waves traveling in the same structure as shown in Figure 3 but built on a ferrite substrate. This goal could be achieved by using the perturbation approach considering the dielectric case as the unperturbed problem, and the ferrite case as the perturbed problem.

A perturbational expression for the propagation constant due to small changes of a material type in a guidance structure is given in reference 8 as

$$\gamma' + \gamma^* = \frac{j\omega \iint_{\Delta S} [(\epsilon_o [\Delta\chi_e] \cdot \bar{E}' \cdot \bar{E}^*) + (\mu_o [\Delta\chi_m] \cdot \bar{H}' \cdot \bar{H}^*)] ds}{\iint_S (\bar{E}^* \times \bar{H}' + \bar{E}' \times \bar{H}^*) \cdot \bar{a}_z ds} \quad (133)$$

where primes denote perturbed quantities.

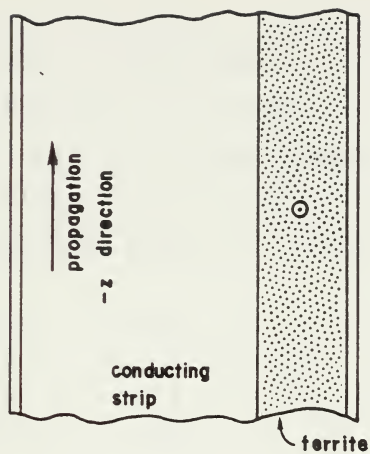
When external magnetic susceptibility is used, and assuming that the dielectric constant remains unchanged, hence $[\Delta\chi_e^e] = 0$ then unperturbed magnetic and electric fields are used instead of the perturbed ones, and equation (133) can be rewritten as

$$\gamma' + \gamma^* = \frac{j\omega\mu_0 \iint_{\Delta S} [\chi_m^e] \cdot \bar{H} \cdot \bar{H}^* ds}{\iint (\bar{E}^* \times \bar{H} + \bar{E} \times \bar{H}^*) \cdot \bar{a}_z ds} \quad (134)$$

In the above equation the following notations are used

γ'	$= \alpha' + j\beta'$	perturbed propagation constant
γ	$= \alpha + j\beta$	unperturbed propagation constant
ΔS		cross section of waveguide which is perturbed by a change of the material type
S		waveguide cross section
χ_m^e		external magnetic susceptibility tensor
\bar{H} and \bar{E}		unperturbed magnetic and electric fields

The external D.C. magnetic field is applied perpendicular to the direction of propagation as shown in Figure 11.



Note: the upper wall of waveguide was removed.

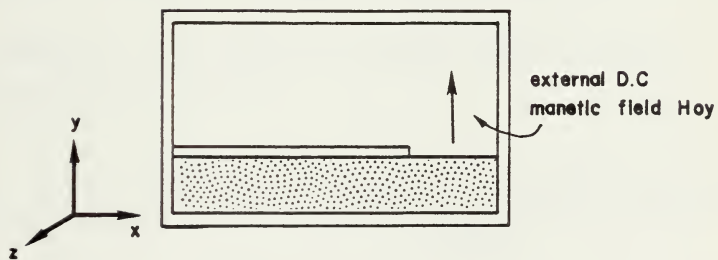


Figure 11. Shielded Isolator Structure.

According to reference 1 the lines of the magnetic field lie in Z-X plane hence an interaction between the R.F. field and the ferrite results when the D.C. magnetic field is applied perpendicular to Z-X plane.

The direction of the applied magnetic field implies no R.F. demagnetization in the y direction. Thus the external magnetic susceptibility tensor is given by

$$[\chi_m^e] = \begin{bmatrix} \chi_{xx} & 0 & \chi_{xz} \\ 0 & 0 & 0 \\ \chi_{zx} & 0 & \chi_{zz} \end{bmatrix} = \begin{matrix} \chi_{xx}\bar{a}_x\bar{a}_x + \chi_{xz}\bar{a}_x\bar{a}_z + \\ + \chi_{zx}\bar{a}_z\bar{a}_x + \chi_{zz}\bar{a}_z\bar{a}_z \end{matrix} \quad (135)$$

and the integrand in the numerator of equation (133) can be explicitly written as

$$[\chi_m^e] \cdot \bar{H} \cdot \bar{H}^* = [\chi_{xx}H_x + \chi_{xz}H_z]H_x^* + [\chi_{zx}H_x + \chi_{zz}H_z]H_z^* \quad (136)$$

The denominator of equation is simply 4Pave so one can rewrite equation (134) as

$$\gamma' + \gamma^* = j\omega\mu_0 \frac{\int_0^D \int_0^A (\chi_{xx}|H_x|^2 + \chi_{zz}|H_z|^2 + \chi_{xz}H_zH_x^* + \chi_{zx}H_xH_z^*) dx dy}{4 \text{ Pave}} \quad (137)$$

B. MAGNETIC SUSCEPTIBILITY TENSOR ELEMENTS

According to small signal approximation of the equation of motion in reference 8 two frequencies can be defined as

$$\omega_z = (\omega_0 - N_y \omega_m + N_z \omega_m) = \omega_0 - \omega_m \quad (138)$$

$$\omega_x = (\omega_0 - N_y \omega_m + N_x \omega_m) = \omega_0 - \omega_m. \quad (139)$$

where

$$\omega_0 = \gamma H_{0y}$$

$$\omega_m = \gamma 4\pi M_s$$

$$\gamma = 1.4 \cdot g [\text{MHz/oe}] = 0.879 \cdot g [\text{Mrad/oe}]$$

g = Lande' factor (≈ 2)

H_{0y} = applied D.C. magnetic field in y direction [oe]

$4\pi M_s$ = saturation magnetization [Gauss]

N_x, N_y, N_z = Demagnetization factors (in this case
 $N_x = N_z = 0, N_y = 1$)

Define the ellipticity of the normal modes of the uniform precession [Ref. 8] as:

$$e_0 = \sqrt{\frac{\omega_x}{\omega_z}} \quad (140)$$

and Kittel resonance relation for an ellipsoid [Refs. 8 and 9] as

$$\omega_r = \sqrt{\omega_x \cdot \omega_z}$$

The Landau-Lifshitz damping factor is defined in reference 9 as

$$\alpha = \frac{\gamma \Delta H}{2\omega} \quad (141)$$

where ΔH is the line width of the ferrite.

In this study the ellipticity e_0 is equal to 1 and $\omega_r = \omega_0 - \omega_m$, so by taking

$$\chi = \chi' - j\chi'' \quad (142)$$

and knowing that [Ref. 8]

$$\chi_{xz} = -\chi_{zx} \quad (143)$$

then the susceptibility elements can be expressed as

$$\chi'_{xx} = \chi'_{zz} = \frac{\omega_m \omega_r (\omega_r^2 - \omega^2) + \omega_m \omega_r \omega^2 \alpha^2}{\Delta} \quad (144)$$

$$\chi''_{xx} = \chi''_{zz} = \frac{\omega_m \omega_r \alpha [\omega_r^2 + \omega^2 (1 + \alpha^2)]}{\Delta} \quad (145)$$

$$\chi'_{xz} = -\chi'_{zx} = j \frac{\omega \cdot \omega_m [\omega_r^2 - \omega^2 (1 + \alpha^2)]}{\Delta} \quad (146)$$

$$\chi''_{xz} = -\chi''_{zx} = j \frac{2\omega^2 \omega_m \omega_r \alpha}{\Delta} \quad (147)$$

and

$$\Delta = [\omega_r^2 - \omega^2 (1 + \alpha^2)]^2 + 4\omega_r^2 \omega^2 \alpha^2 \quad (148)$$

Since $x_{xx} = x_{zz}$ and $x_{xz} = -x_{zx}$ then one can simplify the perturbation expression given in equation (137) as follows

$$\gamma' + \gamma^* = j\omega\mu_0 \frac{\int_0^D \int_0^A [x_{xx} (|H_x|^2 + |H_z|^2) + x_{xz} (H_z H_{yx}^* - H_z^* H_x)]}{4 \text{Pave}} \quad (149)$$

C. COMPUTATION OF PERTURBATION EXPRESSION IN THE SPECTRAL DOMAIN

In order to solve the perturbation expression [Eq. 149], the magnetic fields, H_x and H_z were substituted in terms of the scalar potentials as follows

$$\begin{aligned} \gamma' + \gamma^* = & \frac{j\omega\mu_0}{4\text{Pave}} \int_0^D \int_0^A \left\{ x_{xx} \left[(\pm j\beta \frac{\partial \phi_2^h(x,y)}{\partial x} + j\omega\epsilon_2 \frac{\partial \phi_2^e(x,y)}{\partial y}) \right. \right. \\ & \left. \left. (\mp j\beta \frac{\partial \phi_2^h(x,y)}{\partial x} - j\omega\epsilon_2 \frac{\partial \phi_2^e(x,y)}{\partial y}) + Kc_2^4 \phi_2^h(x,y)^2 \right] + \right. \\ & \left. + 2x_{xz} [Kc_2^2 \phi_2^h(x,y) (\mp j\beta \frac{\partial \phi_2^h(x,y)}{\partial x} - j\omega\epsilon_2 \frac{\partial \phi_2^e(x,y)}{\partial y})] \right\} dx dy. \end{aligned} \quad (150)$$

The upper and lower signs denote waves traveling in negative and positive z-directions respectively.

Apply Parseval's theorem

$$\begin{aligned} \gamma' + \gamma^* = & \frac{j\omega\mu_0}{4\text{Pave}A} \sum_{n=-\infty}^{n=\infty} \int_0^D \left\{ x_{xx} [(\beta^2 \alpha_n^2 + Kc_2^4) |\phi_2^h(\alpha_n, y)|^2 + \right. \\ & \left. \mp j\beta \alpha_n \omega \epsilon_2 (\phi_2^h(\alpha_n, y) \frac{\partial \phi_2^{e*}(\alpha_n, y)}{\partial y} - \phi_2^{h*}(\alpha_n, y) \frac{\partial \phi_2^e(\alpha_n, y)}{\partial y}) + \right. \end{aligned} \quad (151)$$

$$+ \omega^2 \epsilon_2^2 \left| \frac{\partial \phi_2^e(\alpha n, y)}{\partial y} \right|^2 + \quad (151)$$

$$+ 2\chi_{xz} K c_2^2 \phi_2^h(\alpha n, y) \left[\pm \beta \alpha n \phi_2^{h*}(\alpha n, y) - j \omega \epsilon_2 \frac{\partial \phi_2^{e*}}{\partial y} \right] \Big\} dy.$$

The integration with respect to y was computed analytically for both regions where γ_2 is either a real or an imaginary quantity.

Recall equations (49) through (52)

$$\phi_2^h(\alpha n, y) = \begin{cases} C_H^h(\alpha n) \cosh \gamma_2 y & \gamma_2 \text{ real} \\ C_T^h(\alpha n) \cos \gamma_2 y & \gamma_2 \text{ imaginary} \end{cases}$$

$$\frac{\partial \phi_2^e(\alpha n, y)}{\partial y} = \begin{cases} \gamma_2 D_H^e(\alpha n) \cosh \gamma_2 y & \gamma_2 \text{ real} \\ \gamma_2 D_T^e(\alpha n) \cos \gamma_2 y & \gamma_2 \text{ imaginary.} \end{cases}$$

Substituting into equation (151) for both hyperbolic and trigonometric cases, and integrating with respect to y , one can obtain:

For the hyperbolic case (152)

$$\begin{aligned} \gamma' + \gamma^* = & \frac{j \omega \mu_0}{8 P_{ave} A} \sum_{n=-\infty}^{n=\infty} \left\{ \chi_{xx} \left[\frac{\sinh 2\gamma_2 D}{2\gamma_2} + D \right] \left[(\beta^2 \alpha n^2 + K c_2^2) |C_H^h(\alpha n)|^2 + \right. \right. \\ & + \omega^2 \epsilon_2^2 \gamma_2^2 |D_H^e(\alpha n)|^2 + j \beta \alpha n \omega \gamma_2 \epsilon_2 (C_H^h(\alpha n) D_H^{e*}(\alpha n) - \\ & - C_H^{h*}(\alpha n) D_H^e(\alpha n)) \Big] - \\ & \left. - j 2 \chi_{xz} K c_2^2 \omega \epsilon_2 \gamma_2 D_H^{e*}(\alpha n) C_H^h(\alpha n) \left[\frac{\sinh 2\gamma_2 D}{2\gamma_2} + D \right] \right\} \end{aligned}$$

And similarly for the trigonometric case

(153)

$$\begin{aligned} \gamma' + \gamma^* = & \frac{j\omega\mu_0}{8P_{ave}A} \sum_{n=-\infty}^{\infty} \left\{ \chi_{xx} \left[\frac{\sin 2\gamma_2'' D}{2\gamma_2''} + D \right] [(\beta^2 \alpha n^2 + Kc_2^2) \cdot |C_T^h(\alpha n)|^2 \right. \\ & + \omega^2 \epsilon_2^2 \gamma_2''^2 |D_T^e(\alpha n)|^2 + \beta \alpha n \omega \epsilon_2 \gamma_2'' (C_T^h(\alpha n) D_T^{e*}(\alpha n) + \\ & \left. + C_T^{h*}(\alpha n) D_T^e(\alpha n))] - \right. \\ & \left. - 2\chi_{xz} Kc_2^2 \omega \epsilon_2 \gamma_2'' D_T^{e*}(\alpha n) C_T^h(\alpha n) \left[\frac{\sin 2\gamma_2'' D}{2\gamma_2''} + D \right] \right\}. \end{aligned}$$

D. COMPUTATION OF NORMALIZED PHASE CONSTANT AND ATTENUATION

The perturbed and unperturbed propagation constants have the form of

$$\gamma' = \alpha' + j\beta' \quad (154)$$

$$\gamma = j\beta \quad (\alpha = 0 \text{ for dielectric case})$$

Thus the left hand side of the perturbation expression is equal to

$$\gamma' + \gamma^* = \alpha' + j\beta' + (-j\beta) = \alpha' + j(\beta' - \beta) \quad (155)$$

Using equation (155) one can obtain

$$\alpha' + j(\beta' - \beta) = \frac{j\omega\mu_0}{8P_{ave} \cdot A} \sum_{n=-\infty}^{\infty} (R_E + jI_m) \quad (156)$$

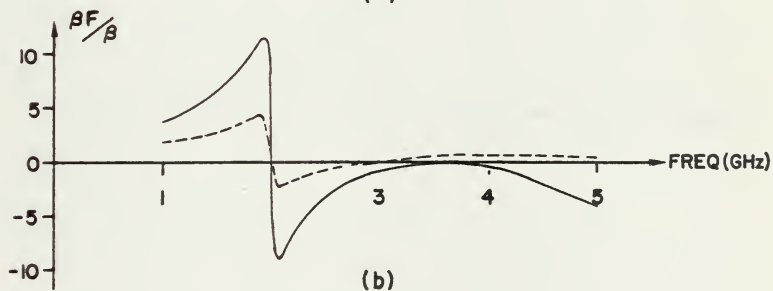
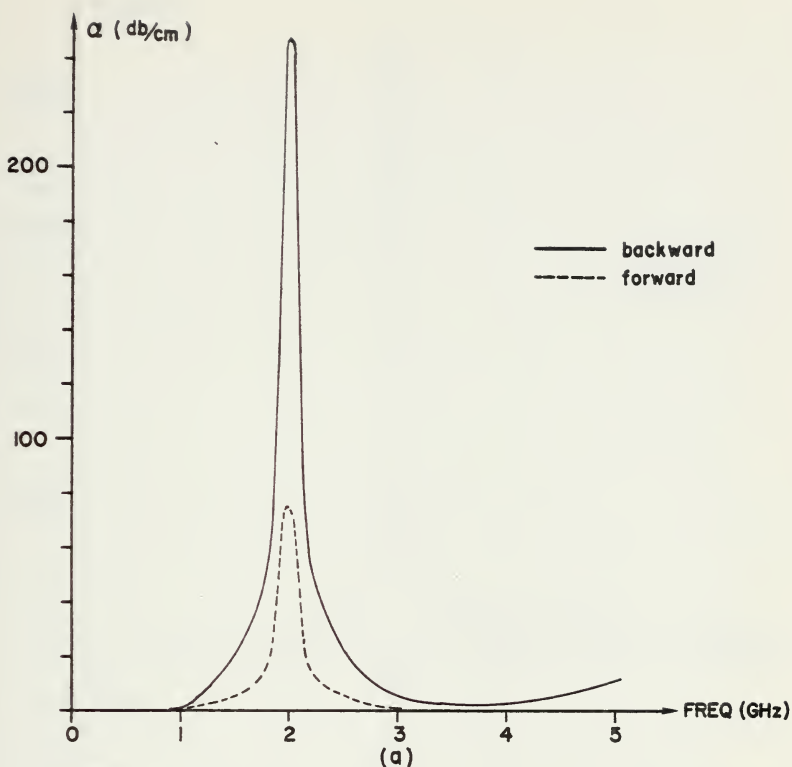


Figure 12. a) Attenuation and
 b) Normalized Propagation Constant for Waves
 Traveling in +Z and -Z Directions for:
 $\Delta H = 75$ oe., $H_{D.C.} = 1916.3$ oe,
 $4\pi MS = 1200$ Ga, $g = 1.99$ $\epsilon_r = 15.2$

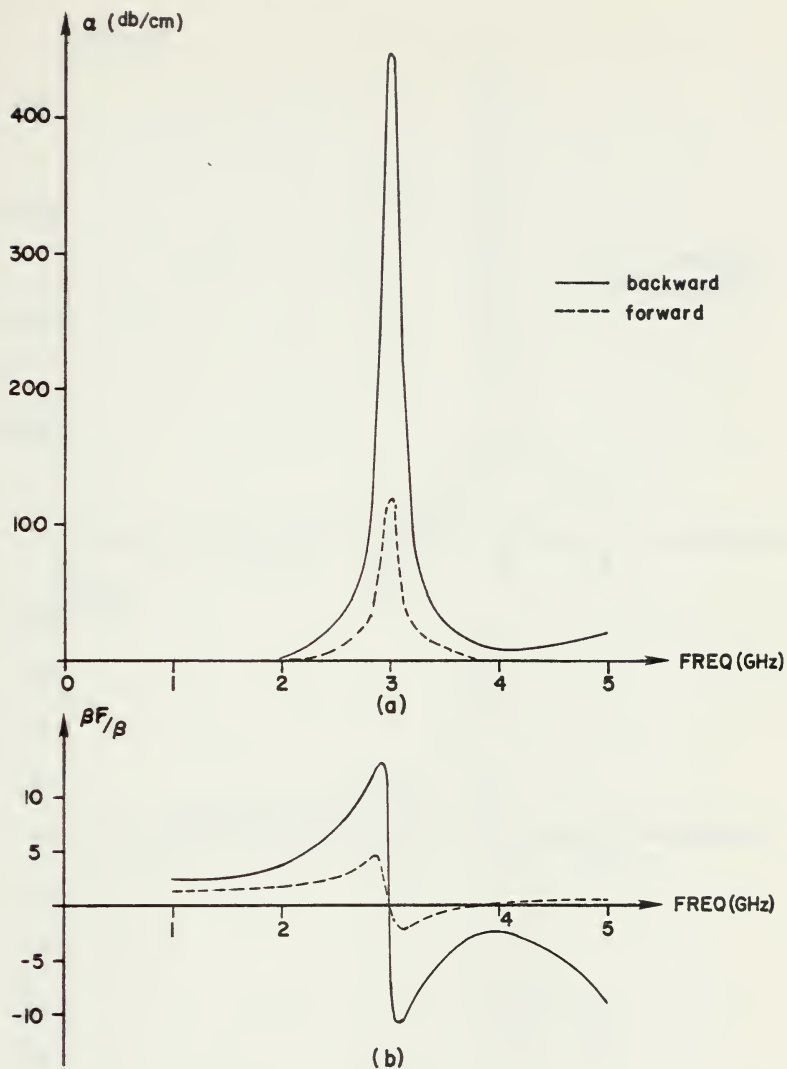


Figure 13. a) Attenuation and
 b) Normalized Propagation Constant for Waves
 Traveling in +Z and -Z Directions for:
 $\Delta H = 750e$, $H_D = 2271.420e$,
 $4\pi MS = 1200$ Ga $C_g = 1.99$, $\epsilon_r = 15.2$

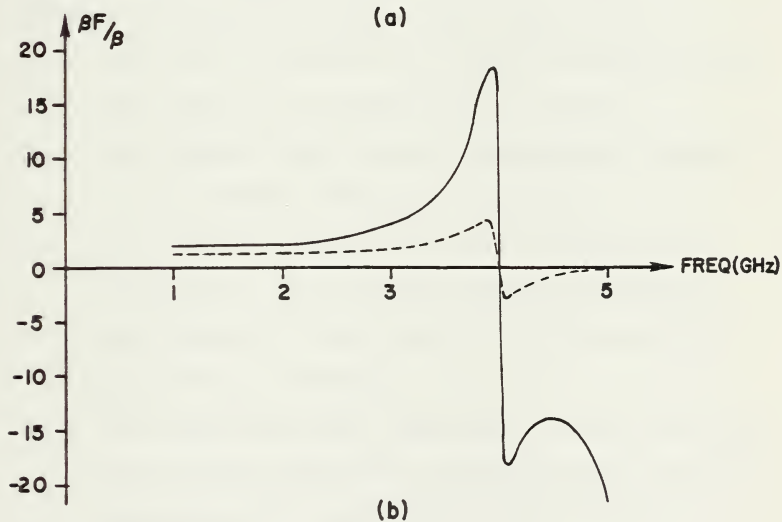
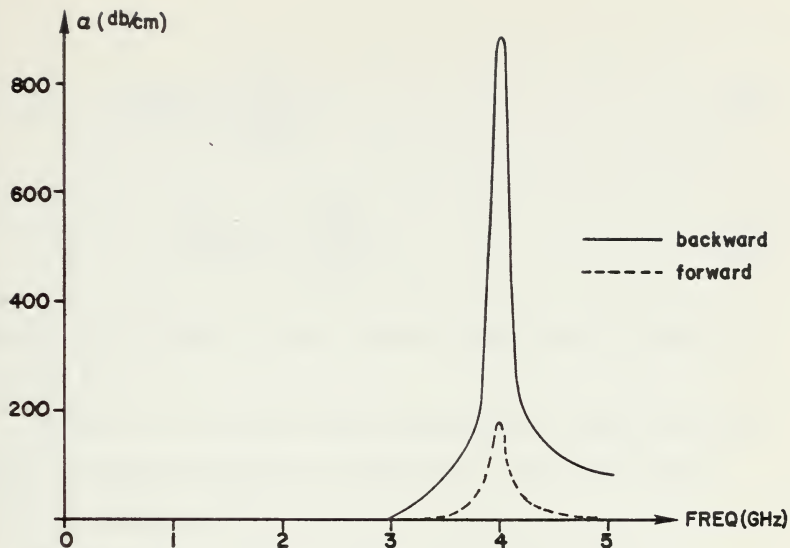


Figure 14. a) Attenuation and
 b) Normalized Propagation Constant for Waves
 Traveling in +Z and -Z Directions for:
 $\Delta H = 75$ oe, $H_{D.C} = 2628.6$ oe,
 $4\pi MS = 1200$ Ga, $g = 1.99$, $\epsilon_r = 15.2$

or

$$\alpha' = - \frac{\omega \mu_0}{8P_{ave} \cdot A} \sum_{n=-\infty}^{\infty} I_m \quad (157)$$

$$\beta'/\beta = 1 + \frac{\omega \mu_0}{8P_{ave} A \cdot \beta} \sum_{n=-\infty}^{\infty} R_E \quad (158)$$

Detailed development of the last two equations is given in appendix B.

Figures 12, 13 and 14 were plotted for three different values of external magnetic fields H_{oy} , hence for three different resonant frequencies.

Several facts can be studied from these plots.

- a. The ratio of backward to forward attenuation is very large, as required for an isolator.
- b. Both backward and forward attenuations increase as the resonant frequency increases.
- c. The ratio of backward to forward attenuation increases as the resonant frequency increases.
- d. The bandwidth of the isolator is determined by the ferrite linewidth.
- e. The normalized phase constants in both directions are frequency dependent and exceed high values as approaching the lower side of the isolator's bandwidth.

The region of negative values of normalized phase constants was not investigated, thus at present no explanation is obtained. Hopefully laboratory measurements will indicate whether it was an error due to the inherent approximations of the perturbational technique, or how large are the deviations from the correct results.

IV. COMPUTER PROGRAMMING

The computer program that was developed for this study was written in FORTRAN IV language and has three major steps:

1. Computing wavelength ratio λ'/λ , for waves traveling in a device built on dielectric substrate (Fig. 3).
2. Computing power flow in a device built on dielectric substrate.
3. Computing normalized phase constant $\beta F/\beta$, and attenuation in db/cm for waves traveling in a device built on ferrite substrate (Fig. 3).

These computations were done for both forward and backward directions of propagation.

The computations of the wavelength ratio in step 1 were made by finding the root β that solved the determinantal equation (113). First, equation (113) was solved for an arbitrary value of β , and then, by the use of Newton-Raphson iteration method, β was computed until the change between two β 's in two successive iterations was in the 6th or 7th digit after the decimal point. From the value of the last β , λ'/λ could easily be computed.

In step 2 the power flow was computed for both hyperbolic and trigonometric cases, depending whether γ_2 was a real or imaginary quantity. The computed β , and the coefficient ratio a_2/a_1 obtained in part 1, were used as entries in part 2.

In step 3 both power flow and computed β were used as entries. This step was executed twice each time for waves traveling in both directions. The output of this step could be obtained for only one value of the following parameter at each run:

Ferrite linewidth
Applied D.C. magnetic field
Saturation magnetization and
Landé'-g of the ferrite.

All three steps could be calculated for different values of frequencies strip's width and substrate's thickness in one run.

The required input data to the program is given in Appendix C.

The limits for all summations in the program were chosen by a trial and error method, since there were no definite limits that could be pointed out.

The upper and lower frequencies of operation are bounded as follows.

Lower frequency is bounded by the strip's width such as

$$\frac{\lambda_0 \max}{4\sqrt{\epsilon r_2}} = W \quad (159)$$

or

$$f_{\min} = \frac{C}{4W\sqrt{\epsilon r_2}} \quad (160)$$

Approximated upper bound was applied according to reference 10. This reference discusses the case of a rectangular guide with dielectric slab perpendicular to the electric field as shown in Figure 15.

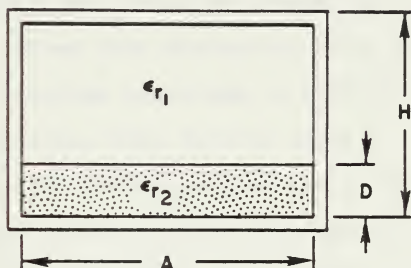


Figure 15. Waveguide Filled with Dielectric Slab Perpendicular to the Electric Field.

The guided wavelength is given as

$$\lambda_g = \frac{\lambda_0}{\sqrt{\frac{\epsilon r_1}{1 - \frac{D}{H}(1 - \frac{\epsilon r_1}{\epsilon r_2})} - \left(\frac{\lambda_0}{2A}\right)^2}} \quad (161)$$

The cut-off wavelength of this guide is the one that set the denominator equal to zero, so from equation (161) one can obtain

$$\lambda_{0 \text{ min}} = 2A \sqrt{\frac{\epsilon r_1}{1 - \frac{D}{H}(1 - \frac{\epsilon r_1}{\epsilon r_2})}} \quad (162)$$

and

$$f_{\text{max}} = \frac{c}{\lambda_{0 \text{ min}}} \quad (163)$$

V. CONCLUSIONS

In this study a theoretical analysis of a model for a shielded edge-guided mode isolator was presented.

The analysis was based on a complete solution for an unperturbed problem (the dielectric case) and then by the use of a perturbation technique, a solution was derived for a perturbed problem, (the ferrite case).

Final results indicated that above and below the resonant frequency the forward attenuation is very low - negligible, while the reverse attenuation is high. These are good regions in which to operate as an isolator. One result which is still unexplained is that the normalized phase constant is negative in the frequency region above the resonant frequency.

A computer program was developed for all steps of the theoretical analysis.

APPENDIX A

AVERAGE POWER FLOW IN REGIONS 1 and 2

Equation (129) indicates the total power flow in region 1. In order to solve this equation both \bar{A}^e and \bar{A}^h should be known explicitly.

Recall

$$\bar{A}^e(n) = \frac{E_z(\alpha n)}{Kc_1^2 \sinh \gamma_1 (D-H)} \quad (A-1)$$

$$\bar{A}^h(\alpha n) = -j \left[\frac{\alpha n \beta E_z(\alpha n)}{Kc_1^2} - E_x(\alpha n) \right] \frac{1}{\omega \mu_1 \gamma_1 \sinh \gamma_1 (D-H)} \quad (A-2)$$

$$E_x(\alpha n) = M_1^{H,T}(\alpha n, \beta) J_x(\alpha n) + M_2^{H,T}(\alpha n, \beta) J_z(\alpha n) \quad (A-3)$$

$$E_z(\alpha n) = M_3^{H,T}(\alpha n, \beta) J_x(\alpha n) + M_4^{H,T}(\alpha n, \beta) J_z(\alpha n) \quad (A-4)$$

Since $M_1^{H,T}(\alpha n, \beta)$, $M_2^{H,T}(\alpha n, \beta)$, $M_3^{H,T}(\alpha n, \beta)$ and $M_4^{H,T}(\alpha n, \beta)$ are imaginary quantities, one can define

$$M_1^{H,T}(\alpha n, \beta) = jm_1^{H,T}(\alpha n, \beta)$$

$$M_2^{H,T}(\alpha n, \beta) = jm_2^{H,T}(\alpha n, \beta)$$

$$M_3^{H,T}(\alpha n, \beta) = jm_3^{H,T}(\alpha n, \beta)$$

$$M_4^{H,T}(\alpha n, \beta) = jm_4^{H,T}(\alpha n, \beta)$$

(A-5)

Furthermore, referring to equation (115) one can assume that a_2 is a real quantity and a_1 is imaginary quantity. So one can write .

$$a_1 = j\bar{a}_1 \quad (\text{A-6})$$

where \bar{a}_1 is real quantity.

Substituting equation (A-5), (A-6), (110) and (111) into equations (A-3) and (A-4) one can obtain

$$E_x(\alpha n) = E_{x_1}(\alpha n) + jE_{x_2}(\alpha n) \quad (\text{A-7})$$

$$E_z(\alpha n) = E_{z_1}(\alpha n) + jE_{z_2}(\alpha n) \quad (\text{A-8})$$

where

$$E_{x_1}(\alpha n) = \bar{a}_1 \left[-\frac{a_2}{\bar{a}_1} m_1^{H,T}(\alpha n, \beta) g_{x_0}(\alpha n) - m_2^{H,T}(\alpha n, \beta) f_{z_e}(\alpha n) \right] \quad (\text{A-9})$$

$$E_{x_2}(\alpha n) = \bar{a}_1 \left[\frac{a_2}{\bar{a}_1} \cdot m_1^{H,T}(\alpha n, \beta) g_{x_e}(\alpha n) - m_2^{H,T}(\alpha n, \beta) f_{z_0}(\alpha n) \right] \quad (\text{A-10})$$

$$E_{z_1}(\alpha n) = \bar{a}_1 \left[-\frac{a_2}{\bar{a}_1} m_3^{H,T}(\alpha n, \beta) g_{x_0}(\alpha n) - m_4^{H,T}(\alpha n, \beta) f_{z_e}(\alpha n) \right] \quad (\text{A-11})$$

$$E_{z_2}(\alpha n) = \bar{a}_1 \left[\frac{a_2}{\bar{a}_1} m_3^{H,T}(\alpha n, \beta) g_{x_e}(\alpha n) - \right. \\ \left. - m_4^{H,T}(\alpha n, \beta) f_{z_0}(\alpha n) \right] \quad (A-12)$$

and

$$\frac{a_2}{\bar{a}_1} = \frac{\sum_{n=-\infty}^{\infty} m_2^{H,T}(\alpha n, \beta) B(\alpha n)}{\sum_{n=-\infty}^{\infty} m_1^{H,T}(\alpha n, \beta) |g_x(\alpha n)|^2} \quad (A-13)$$

After investigating equations (A-9) through (A-12) it could be seen that $E_{x_1}(\alpha n)$ and $E_{z_2}(\alpha n)$ are even functions, while $E_{x_2}(\alpha n)$ and $E_{z_1}(\alpha n)$ were odd functions. Substitution of these functions into equations (A-1) and (A-2) led to explicit expressions of $\bar{A}^e(\alpha n)$ and $\bar{A}^h(\alpha n)$, hence the power flow in region 1 could be calculated.

It is clear that the power flow in region 2 for both the hyperbolic and trigonometric cases could be calculated in the same way since the coefficients $D_H^e(\alpha n)$, $C_H^h(\alpha n)$, $D_T^e(\alpha n)$ and $C_T^h(\alpha n)$ are functions of $E_x(\alpha n)$ and $E_z(\alpha n)$ which their explicit expressions are given in equations (A-9) through (A-12).

APPENDIX B

NORMALIZED PHASE CONSTANT AND ATTENUATION

As was stated in equation (157) and (158)

$$\alpha' = - \frac{\omega \mu_0}{8P_{ave}A} \sum_{n=-\infty}^{\infty} I_m \quad (B-1)$$

$$\beta'/\beta = 1 + \frac{\omega \mu_0}{8P_{ave}A} \sum_{n=-\infty}^{\infty} R_E \quad (B-2)$$

So in order to calculate α' and β'/β , both I_m and R_E should be known explicitly.

For the hyperbolic case, equation (151) had to be divided into real and imaginary components.

Recall equations (67) and (68) and substrate equations (A-7) and (A-8) for $E_x(\alpha n)$ and $E_z(\alpha n)$ one can obtain

$$C_H^h(\alpha n) = \frac{1}{\omega \mu_2 \gamma_2 \sinh \gamma_2 D} \left\{ \left[- \frac{\beta \alpha_n}{Kc_2} E_{z_2}(\alpha n) + E_{x_2}(\alpha n) \right] + \right. \quad (B-3)$$

$$\left. + j \left[\frac{\beta \alpha_n}{Kc_2} E_{z_1}(\alpha n) - E_{x_1}(\alpha n) \right] \right\}$$

$$D_H^e(\alpha n) = \frac{1}{Kc_2 \sinh \gamma_2 D} [E_{z_1}(\alpha n) + jE_{z_2}(\alpha n)] \quad (B-4)$$

Substituting equations (B-3) and (B-4) into equation (152) and separating to real and imaginary parts, the following equations are obtained

$$\begin{aligned}
 RI_1 = & \frac{\beta^2 \alpha n^2 + Kc_2^2}{\omega^2 \mu_2^2 \gamma_2^2} \left\{ \left[-\frac{\beta \alpha n}{K_2} E_{z_2}(\alpha n) + E_{x_2}(\alpha n) \right]^2 + \right. & (B-5) \\
 & + \left. \left[\frac{\beta \alpha n}{Kc_2} E_{z_1}(\alpha n) - E_{x_1}(\alpha n) \right]^2 \right\} + \\
 & + \frac{\omega^2 \epsilon_2^2 \gamma_2^2}{Kc_2^4} [E_{z_1}^2(\alpha n) + E_{z_2}^2(\alpha n)] + \\
 & + \frac{2\beta \alpha n}{Kc_2} \left\{ \frac{\beta \alpha n}{K_2} [E_{z_1}^2(\alpha n) + E_{z_2}^2(\alpha n)] - \right. \\
 & \left. - E_{z_1}(\alpha n)E_{x_1}(\alpha n) - E_{z_2}(\alpha n)E_{x_2}(\alpha n) \right\}
 \end{aligned}$$

$$RI_2 = \frac{\epsilon_2}{\mu_2} [E_{x_1}(\alpha n)E_{z_2}(\alpha n) - E_{x_2}(\alpha n)E_{z_1}(\alpha n)] \quad (B-6)$$

$$RE = \left[\frac{\text{ctgh} \gamma_2 D}{\gamma_2} + \frac{D}{\sinh^2 \gamma_2 D} \right] \left[\frac{X'_{xx}}{2} RI_1 + \frac{X'_{xz}}{2} RI_2 \right] \quad (B-7)$$

$$Im = \left[\frac{\text{ctgh} \gamma_2 D}{\gamma_2} + \frac{D}{\sinh^2 \gamma_2 D} \right] \left[-\frac{X''_{xx}}{2} RI_1 - \frac{X''_{xz}}{2} RI_2 \right] \quad (B-8)$$

Similarity for the trigonometric case the coefficients $C_T^h(\alpha n)$ and $D_T^e(\alpha n)$ can be expressed in terms of $E_{X_1}(\alpha n)$ and $E_{Z_2}(\alpha n)$ as follows

$$C_T^h(\alpha n) = \frac{1}{\omega \mu_2 \gamma_2^2 \sin^2 \gamma_2 D} \left\{ \left[\frac{\beta \alpha n}{Kc_2} E_{Z_2}(\alpha n) - E_{X_2}(\alpha n) \right] + \right. \quad (B-9)$$

$$\left. + j \left[- \frac{\beta \alpha n}{Kc_2} E_{Z_1}(\alpha n) + E_{X_1}(\alpha n) \right] \right\}$$

$$D_T^e(\alpha n) = -j \frac{1}{Kc_2 \sin^2 \gamma_2 D} E_{Z_2}(\alpha n) \quad (B-10)$$

and both the real and imaginary parts of equation (152) have the form of

$$RI_1 = \frac{\beta^2 \alpha n^2 + Kc_2^2}{\omega^2 \mu_2^2 \gamma_2^2} \left\{ \left[\frac{\beta \alpha n}{Kc_2} E_{Z_2}(\alpha n) - E_{X_2}(\alpha n) \right]^2 + \right. \quad (B-11)$$

$$\left. + \left[- \frac{\beta \alpha n}{Kc_2} E_{Z_1}(\alpha n) + E_{X_1}(\alpha n) \right]^2 \right\} +$$

$$+ \frac{\omega^2 \epsilon_2 \gamma_2^2}{Kc_2^4} [E_{Z_1}^2(\alpha n) + E_{Z_2}^2(\alpha n)] +$$

$$+ \frac{2\beta \alpha n}{Kc_2} \left\{ \frac{\beta \alpha n}{Kc_2} [E_{Z_1}^2(\alpha n) + E_{Z_2}^2(\alpha n)] - \right.$$

$$\left. - E_{Z_1}(\alpha n)E_{X_1}(\alpha n) - E_{Z_2}(\alpha n)E_{X_2}(\alpha n) \right\}$$

$$RI_2 = -\frac{\epsilon_2}{\mu_2} [E_{x_1}(\alpha n)E_{z_2}(\alpha n) - E_{x_2}(\alpha n)E_{z_1}(\alpha n)] \quad (B-12)$$

$$R_E = \left[\frac{D}{\sin^2 \gamma_2''} + \frac{\text{ctg} \gamma_2'' D}{\gamma_2''} \right] \left[\frac{\chi_{xx}'}{2} RI_1 + \frac{\chi_{xz}'}{2} RI_2 \right] \quad (B-13)$$

$$I_m = \left[\frac{D}{\sin^2 \gamma_2''} + \frac{\text{ctg} \gamma_2'' D}{\gamma_2''} \right] \left[-\frac{\chi_{xx}''}{2} RI_1 - \frac{\chi_{xz}''}{2} RI_2 \right] \quad (B-14)$$

After substituting properly equations (B-7), (B-8), (B-13) and (B-14) into equations (B-1) and (B-2) the later can be solved for the attenuation and normalized phase constant.

APPENDIX C
COMPUTER PROGRAM

THEORY OF FIELD DISPLACEMENT DEVICES

SHIELDED EDGE GUIDED MODE ISOLATOR
(BOX'S DIMENSION 0.4''*0.9'')

THIS PROGRAM HAS THREE MAJOR STEPS CORRESPONDING TO THE STEPS OF THE THEORETICAL ANALYSIS OF THE DEVICE. THE THREE STEPS ARE:

1. COMPUTING WAVELENGTH RATIO OF THE DEVICE BUILT ON DIELECTRIC SUBSTRATE.
2. COMPUTING POWER FLOW IN THE DEVICE.
3. COMPUTING NORMALIZED PROPAGATION CONSTANT AND ATTENUATION IN DB PER CM OF FERRITE BUILT DEVICE BY USING PERTURBATION THEORY AND DATA OBTAINED IN STEPS 1 & 2.

PROGRAM ACCEPTS FOLLOWING DATA:

1. FIRST CARD-(L1,M1,MN1) FORMAT(3(I2,X2))
L1 -NUMBER OF FREQ. DATA CARDS.
M1 -NUMBER OF STRIP WIDTHS DATA CARDS.
MN1-NUMBER OF SUBSTRATE THICKNESS DATA CARDS.
2. SECOND CARD-(FREQ(L),L=1,L1) FORMAT(D9.3)
FREQ(L) ARE THE FREQUENCIES IN HERTZ AT WHICH THE COMPUTATIONS ARE EXECUTED.
NUMBER OF "SECOND" CARDS=L1.
3. THIRD CARD-(W(M),M=1,M1) FORMAT(D10.4)
W(M) ARE THE VARIOUS STRIP WIDTHS, IN METERS.
NUMBER OF "THIRD" CARDS=M1.
4. FOURTH CARD-(D(MN),MN=1,MN1) FORMAT(D10.4)
D(MN) ARE THE VARIOUS SUBSTRATE THICKNESS, IN METERS.
NUMBER OF "FOURTH" CARDS=MN1.
5. FIFTH CARD-EPSR FORMAT(F5.2)
EPSR- RELATIVE DIELECTRIC CONSTANT.
6. SIXTH CARD-DELTH FORMAT(D12.3)
DELTH-LINEWIDTH OF FERRITE IN CERSTEDS.
7. SEVENTH CARD-HO FORMAT(D12.3)
HO-APPLIED D.C MAGNETIC FIELD IN OERSTEDS.
8. EIGHTH CARD-AMAGS FORMAT(D12.3)
AMAGS-SATURATION MAGNETIZATION IN GAUSS.
9. NINTH CARD-G FORMAT(F4.2)
G- LANDE-G OF FERRITE.

OUTPUT:

1. WAVELENGTH RATIO FOR DIELECTRIC SUBSTRATE.
2. NORMALIZED PROPAGATION CONSTANT FOR BACKWARD AND FORWARD DIRECTIONS OF PROPAGATION.
3. ATTENUATION FOR BACKWARD AND FORWARD DIRECTIONS OF PROPAGATION.

THE OUTPUT IS PRINTED FOR ALL FREQUENCIES, STRIP WIDTHS AND SUBSTRATE THICKNESS.

CAUTION: THE UPPER AND LOWER FREQUENCIES OF OPERATION ARE BOUNDED TO ELIMINATE UNDESIREED MODES OF

PROPAGATION IN THE DEVICE.

ALL COMPUTATIONS ARE PERFORMED IN DOUBLE PRECISION.

LANGUAGE-FORTRAN

PROGRAM DEVELOPED BY LT. J. G. RAM SHARON ISRAELI NAVY.
 THESIS ADVISOR- PROF. DR. J. B. KNORR.
 NAVAL POSTGRADUATE SCHOOL MONTEREY CALIFORNIA 93940
 FEBRUARY 1976

IMPLICIT REAL*8 (A-H,C-Z)
 DIMENSION TOT(4), FREQ(10), W(8), D(8)

ZZ=20.00
 S=0.00

1 FORMAT (D9.3)
 2 FORMAT (D10.4)
 3 FORMAT (3(I2,2X))
 5 FORMAT (F5.2)
 10 FORMAT (D12.3)
 7 FORMAT (F4.2)

READ (5,3) L1, M1, MN1
 READ (5,1) (FREQ(L), L=1, L1)
 READ (5,2) (W(M), M=1, M1)
 READ (5,2) (D(MN), MN=1, MN1)
 READ (5,5) EPSR
 READ (5,10) DELTH
 READ (5,10) HO
 READ (5,10) AMAGS
 READ (5,7) G

PI=3.14159265400
 AMU1=4.00*PI*1.0D-7
 AMUR=1.00
 AMU2=AMU1*AMUR
 EPS1=1.00/(36.00*PI*1.0+9)
 EPS2=EPS1*EPSR

STEP1-WAVELENGTH RATIO CALCULATIONS.

H-BOX'S HEIGHT

H=1.016D-2

A-BOX'S WIDTH

A=2.286D-2

FREQUENCY LOOP

DO 4000 L=1, L1
 FREQ1=FREQ(L)/1.0D+9
 OMEGA=2.00*PI*FREQ(L)
 OMEGA1=OMEGA/1.0D+9
 WRITE (6,4)
 4 FORMAT (//////////)

PRINT OUT OF INPUT DATA

WRITE (6,199)
 199 FORMAT (30X, 22H*****
 WRITE (6,200) FREQ1
 200 FORMAT (30X, 8H# FREQ1=, F5.3, 7H GRPS, 2H *)
 WRITE (6,201) OMEGA1
 201 FORMAT (30X, 9H# OMEGA1=, F6.3, 5H GRPS, 2H *)
 WRITE (6,202) H
 202 FORMAT (30X, 4H# H=, E11.4, 5H MTR, 2H *)
 WRITE (6,203) A
 203 FORMAT (30X, 4H# A=, E11.4, 5H MTR, 2H *)
 WRITE (6,207) EPSR
 207 FORMAT (30X, 7H# EPSR=, F4.1, 9X, 2H *)

```

WRITE (6,206) DELTH
206 FORMAT (30X,10H* DELTH= ,F7.2,5H CE *)
WRITE (6,210) HO
210 FORMAT (30X,10H* C.C.FLD=,F7.2,5H CE *)
WRITE (6,212) AMAGS
212 FORMAT (30X,10H* SAT.MAG=,F7.2,5H GA *)
WRITE (6,213) G
213 FORMAT (30X,10H* LANDE-G=,F4.2,7X,1H*)
WRITE (6,208)
208 FORMAT (30X,22H*****//)
C
C SET HIGHER FREQUENCY OF OPERATION
GM=2.00*A/DSQRT(1.00-D(MN)/H*(1.00-1.00/EPSR))
FREQU=3.08/GM
IF (FREQ(L).GE.FREQU) GO TO 4000
C
C STRIP WIDTH LOOP
DO 5000 M=1,M1
C
C SET LOWER FREQUENCY OF OPERATION
FREQL=(3.00+08/DSQRT(EPSR))/(4*W(M))
IF (FREQ(L).LE.FREQL) GO TO 5000
WRITE (6,205) W(M)
205 FORMAT (10X,2HW=,F11.5//)
C
C SUBSTRATE THICKNESS LOOP
DO 6000 MN=1,MN1
WRITE (6,209)
209 FORMAT (20X,14HLAMBDA'/LAMBDA,7X,1HC,15X,4HBETA/)
N1=101
I1=201
C
C BETA-PROPAGATION CONSTANT
DBETA=1.00-1
BETA1=300.00
C
1000 TOT(1)=20.00
DO 2000 K=1,2
C
BETA=BETA1
IF (K.EQ.2) GO TO 600
GO TO 700
600 BETA=BETA+DBETA
700 AK1=OMEGA*DSQRT(AMU1*EPS1)
AK2=OMEGA*DSQRT(AMU2*EPS2)
AKC1S=AK1**2-BETA**2
AKC2S=AK2**2-BETA**2
C
SUM1=0.000
SUM2=0.000
SUM3=0.000
TTPWR1=0.00
TTPWR2=0.00
TOTPWR=0.00
GO TO 9
C
16 N1=51
I1=101
9 RE11=0.00
RE22=0.00
ZM11=0.00
ZM21=0.00
N=-N1
C
DO 100 I=1,I1
N=N+1
ALFAN=2.00*PI*N/A
6 GAMMA1=DSQRT(ALFAN**2-4KC1S)

```

```

GAMA2S=ALFAN**2-AKC2S
GAMA2=DSQRT(DABS(GAMA2S))
A1=1.00/DTANH(GAMA1*(H-C(MN)))
A2=0.0MEGA*AMU1*GAMA1
A3=0.0MEGA*AMU2*GAMA2
A4=ALFAN*BETA
A5=0.0MEGA*EPS1*GAMA1/AKC1S
A6=0.0MEGA*EPS2*GAMA2/AKC2S
IF (GAMA2S.GE.0.000) GO TO 20
C
C TRIGONOMETRIC CASE
C
A7=DTAN(GAMA2*D(MN))
F1=-AKC1S*A1/A2+AKC2S/(A7*A3)
F2=A4*A1/A2-A4/(A7*A3)
F3=-F2
F4=A4**2*A1/(A2*AKC1S)-A5*A1-A4**2/(AKC2S*A7*A3)-A6/A7
GO TO 30
C
C HYPERBOLIC CASE
C
20 A8=1.00/DTANH(GAMA2*D(MN))
F1=-AKC1S*A1/A2-AKC2S*A8/A3
F2=A4*A1/A2+A4*A8/A3
F3=-F2
F4=A4**2*A1/(A2*AKC1S)-A5*A1+A4**2*A8/(AKC2S*A3)-A6*A8
30 DN=F1*F4-F2*F3
AM1=F4/DN
AM2=-F2/DN
AM3=-AM2
AM4=F1/DN
SN=DSINH(ALFAN*W(M))
CN=DCOS(ALFAN*W(M))
R1=DEXP(ZZ)
R2=(ZZ/W(M))**2+ALFAN**2
R3=R1*CN
R7=R1*SN
Q=(PI/(2.00*W(M)))**2-ALFAN**2
GX1=PI/(2.00*W(M))*CN/Q
GX2=(PI/(2.00*W(M))*SN+ALFAN)/Q
FZ1=(ZZ/W(M))*(R3-1.00)+ALFAN*R7/R2
FZ2=(-ALFAN*(R3-1.00)+ZZ/W(M)*R7)/R2
IF (DABS(TOT(1)).GE.1.0+01) GO TO 8
C
C STEP 2 -POWER FLOW CALCULATIONS.
C
AMP1=1.0-10
Z1=-SUM2/SUM3
Z3=Z1*GX1
Z2=Z1*GX2
EZ1=AMP1*(AM3*Z2-AM4*FZ1)
EZ2=AMP1*(AM3*Z3-AM4*FZ2)
EX1=AMP1*(-Z2*AM1-AM2*FZ1)
EX2=AMP1*(Z3*AM1-AM2*FZ2)
EZX=EZ1**2+EZ2**2
EXS=EX1**2+EX2**2
IF (S.EQ.1.00) GO TO 18
C
C REGION 1 FREE SPACE
C
V0=GAMA1*(H-C(MN))
V1=0.0MEGA*BETA*EPS1/2.00
V2=1.00/DTANH(V0)*GAMA1
IF (V0.GE.85.00) GO TO 12
V3=(H-C(MN))/((DSINH(V0))**2)
GO TO 11
12 V3=0.00
11 V5=BETA/(2.00*0.0MEGA*AMU1)
V4=ALFAN*BETA/AKC1S
V6=(V4*EZ2-EX2)**2+(-V4*EZ1+EX1)**2
V7=V4*EZX-EZ1*EX1-EZ2*EX2
TR11=-V1*ALFAN**2/(AKC1S**2)*EZX*(V2-V3)
TR12=-V5*ALFAN**2/(GAMA1**2)*V6*(V2+V3)
TR13=-V5*V6*(V2-V3)

```

```

TR14=-V1*(GAMA1**2)/(AKC1S**2)*FZS*(V2+V3)
TR156=ALFAN/(OMEGA*AMU1*AKC1S)*(BETA**2+AK1**2)*V7*V2
PWR1=-(TR11+TR12+TR13+TR14+TR156)/(2.00*A)
IF (GAMA2S.LE.0.00) GO TO 800
C
CC REGION 2 HYPERBOLIC CASE
V10=GAMA2*D(MN)
V11=OMEGA*BETA*EPS2/2.00
V12=1.00/(DTANH(V10)*GAMA2)
IF (V10.GE.170.00) GO TO 14
V13=D(MN)/((DSINH(V10))**2)
GO TO 15
14 V13=0.00
15 V15=BETA/(2.00*OMEGA*AMU2)
V14=ALFAN*BETA/ΔK2S
V16=(V14**2-EX2)**2+(-V14*EZ1+EX1)**2
V17=(V14*EZS-EZ1*EX1-FZ2*EX2)
TR21=-V11*ALFAN**2*EZS/(AKC2S**2)*(V12-V13)
TR22=-V15*ALFAN**2/GAMA2S*V16*(V12+V13)
TR23=-V15*V16*(V12-V13)
TR24=-V11*GAMA2S/(AKC2S**2)*(V12+V13)*EZS
TR256=ALFAN/(OMEGA*AMU2*AKC2S)*(BETA**2+AK2**2)*V17*V12
GO TO 801
C
CC REGION 2 TRIGONOMETRIC CASE
300 V25=1.00/(AKC2S*DSIN(GAMA2*D(MN)))
V20=OMEGA*BETA*EPS2/2.00
V21=OMEGA*BETA*AMU2/2.00
DET1=V25*EZ2
DET2=-V25*EZ1
DETS=DET1**2+DET2**2
V26=ALFAN*BETA*V25/(OMEGA*GAMA2*AMU2)
V27=1.00/(OMEGA*AMU2*GAMA2*DSIN(GAMA2*D(MN)))
CHT1=-V26*EZ2+V27*EX2
CHT2=V26*EZ1-V27*EX1
CHTS=CHT1**2+CHT2**2
V28=DSIN(2.00*GAMA2*D(MN))/(2.00*GAMA2)
TR21=-ALFAN**2*V20*DETS*(D(MN)-V28)
TR22=-ALFAN**2*V21*CHTS*(D(MN)+V28)
TR23=-(GAMA2**2)*V21*CHTS*(D(MN)-V28)
TR24=-(GAMA2**2)*V20*DETS*(D(MN)+V28)
TR256=(BETA**2+AK2**2)*ALFAN/2.00*(DET1*CHT1+DET2*CHT2)
801 PWR2=-(TR21+TR22+TR23+TR24+TR256)/(2.00*A)
C
CC TOTAL POWER FLOW IN FREE SPACE REGION
TTPWR1=TTPWR1+PWR1
C
CC TOTAL POWER FLOW IN DIELECTRIC REGION
TTPWR2=TTPWR2+PWR2
C
CC TOTAL POWER FLOW
TOTPWR=TTPWR+PWR1+PWR2
C
GO TO 100
C
8 FZS=(R1**2-2.00*R3+1.00)/R2
GXS=((PI/(2.00*W(M)))*2+ALFAN**2+ALFAN*PI/W(M)*DSIN
X(ALFAN*W(M)))/Q**2
T1N=AM1*GXS
T2N=AM4*FZS
B=-FZ1*GX2+FZ2*GX1
T3N=AM2*B
SUM1=SUM1+T1N
SUM2=SUM2+T2N
SUM3=SUM3+T3N
100 CONTINUE
C
IF (S.EQ.1.00) GO TO 19
IF (TOTPWR.NE.0.00) GO TO 17

```

```

SUM3SQ=(SUM3)**2
TOT(K)=SUM1*SUM2+SUM3SQ
IF (DABS(TOT(1)).LE.1.0+C1) GO TO 3000
C 2000 CONTINUE
C
DTOT=(TOT(2)-TOT(1))/DBETA
BETA1=DABS(BETA1-TOT(1)/DTOT)
60 IF (BETA1.LE.AK1) GO TO 50
GO TO 70
50 BETA1=BETA1+1.00
GO TO 60
70 GO TO 1000
3000 WVLNG=3.00+8/FREQ(L)
RATIO=2.00*PI/(BETA1*WVLNG)
WRITE (6,211) RATIO,D(MN),BETA
211 FORMAT (24X,F6.4,7X,E11.5,7X,E11.5)
GO TO 16
17 S=1.00
C
C SIGN=-1.00 , PROPAGATION IN BACKWARD DIRECTION (+Z)
C
SIGN=-1.00
8000 N1=101
I1=201
GO TO 9
21 S=0.00
6000 CONTINUE
5000 CONTINUE
4000 CONTINUE
C
GO TO 8001
C
C STEP3- CALCULATIONS OF NORMALIZED PROPAGATION CONSTANTS
C AND ATTENUATIONS.
C
18 V14=BETA*ALFAN/AKC2S
V16=(V14*EZ2-EX2)**2+(-V14*EZ1+EX1)**2
V17=(V14*EZ5-EZ1*EX1-EZ2*EX2)
V30=(BETA*ALFAN)**2+AKC2S**2
V31=(OMEGA*AMU2*GAMA2)**2
V32=(OMEGA*EPS2*GAMA2)**2
V33=V30/V31*V16+V32/AKC2S**2*EZ5
V34=(-SIGN)*2.00*V14*EPS2/AMU2*V17
V45=EPS2/AMU2*(EX1*EZ2-EX2*EZ1)
IF (GAMA2S.LE.0.00) GO TO 22
C
C HYPERBOLIC CASE
C
V10=GAMA2*D(MN)
V12=1.00/(DTANH(V10)*GAMA2)
IF (V10.GE.170.00) GO TO 24
V13=D(MN)/((DSINH(V10))**2)
GO TO 25
24 V13=0.00
25 RE1=(V33+V34)*(V12+V13)/2.00
ZM1=-RE1
RE3=V45*(V12+V13)
ZM2=-RE3
GO TO 23
C
C TRIGONOMETRIC CASE
C
22 V40=D(MN)/(DSIN(GAMA2*D(MN))**2)
V41=1.00/(DTAN(GAMA2*D(MN))*GAMA2)
RE1=(V33-V34)*(V40+V41)/2.00
ZM1=-RE1
RE3=-V45*(V40+V41)
ZM2=-RE3
23 RE11=RE11+RE1
RE22=RE22+RE3
ZM11=ZM11+ZM1
ZM21=ZM21+ZM2
GO TO 100
C

```

```

19 G1=2.3D6*PI*G
   CMGAM=G1*AMAGS
   CMGA0=G1*HO
   CMGAR=CMGA0-CMGAM
   DAMP=G1*DELTH/(2.DO*OMEGA)
   DELT=(CMGAR**2-OMEGA**2*(1.DO+DAMP**2))**2+
   X4.DO*(CMGAR*OMEGA*DAMP)**2
C
C
C CALCULATION OF SUSCEPTIBILITY TENSOR'S COMPONENTS
   XXX1=CMGAM*CMGAR*((CMGAR**2-OMEGA**2)+(OMEGA*DAMP)**2)
   XXX2=CMGAM*OMEGA*DAMP*(CMGAR**2+OMEGA**2*(1.DO+DAMP**2))
   XXZ1=OMEGA*CMGAM*(CMGAR**2-OMEGA**2*(1.DO+DAMP**2))
   XXZ2=2.DO*OMEGA**2*CMGAM*DAMP*CMGAR
   RE=XXX1*RE11+RE22*XXZ1
   ZM=XXX2*ZM11+ZM21*XXZ2
904 FORMAT (///)
   WRITE (6,504)
   WRITE (6,904)
C
   V50=OMEGA*AMU1/(4.DO*TOTPWR*DELT*A)
   ATTEN=-ZM*V50
   DB=8.685889638D-02*ATTEN
   BETAP=BETA1+RE*V50
   RAT=BETAP/BETA
   IF (SIGN.EQ.1.DO) GO TO 81
   WRITE (6,898) DB
858 FORMAT (10X,21HBACKWARD ATTENUATION=,E11.5,6H DB/CM//)
   WRITE (6,897) RAT
857 FORMAT (10X,21HBETAF/BETA BACKWARD =,E10.4//)
C
C
C SIGN=+1.DO ,PROPAGATION IN FORWARD DIRECTION (-Z)
   SIGN=+1.DO
   GO TO 8000
81 WRITE (6,900) DB
900 FORMAT (10X,20HFORWARD ATTENUATION=,E11.5,6H DB/CM//)
   WRITE (6,899) RAT
899 FORMAT (10X,20HBETAF/BETA FORWARD =,E10.4//)
   GO TO 21
C
8001 STOP
   END

```

LIST OF REFERENCES

1. M. E. Hines, "Reciprocal and Nonreciprocal Modes of Propagation in Ferrite Stripline and Microstrip Devices," IEEE Trans. Microwave Theory and Techniques, Vol. MTT-19, p. 442-447, May 1971.
2. K. Araki, T. Koyama and Y. Naito, "A New Type of Isolator Using the Edge-Guided Mode," IEEE Trans. Microwave Theory and Techniques, Vol. MTT-23, p. 321, March 1975.
3. T. Itoh and R. Mittra, "Spectral-Domain Approach for Calculating the Dispersion Characteristics of Microstrip Lines," IEEE Trans. Microwave Theory and Techniques, Vol. MTT-21, p. 496-499, July 1973.
4. K. D. Kuchler, Hybrid Mode Analysis of Coplanar Transmission Lines, Ph.D Thesis, Naval Postgraduate School, Monterey, California, 1975.
5. A. M. Tüfekcioğlu, Hybrid Mode Analysis of Microstrip on Dielectric and Ferrite Substrate, Engineer Thesis, Naval Postgraduate School, Monterey, California, 1974.
6. A. B. Carlson, Communication Systems and Introduction to Signals and Noise in Electrical Communication, 2nd ed., p. 71-72, McGraw-Hill, 1975.
7. Reference Data for Radio Engineers, 5th ed., Ch. 44, p. 2, Howard W. Sons & Co., Inc. 1976.
8. J. Helszajn, Principle of Microwave Ferrite Engineering, p. 3-16 and p. 129, J. Wiley & Sons, Ltd., 1969.
9. B. Lax and K. J. Button, Microwave Ferrites and Ferrimagnetics, p. 147-164, McGraw-Hill, 1962.
10. N. Marcuwitz, Waveguide Handbook, 1st ed., p. 391-393, McGraw-Hill, 1951.

INITIAL DISTRIBUTION LIST

		No. Copies
1.	Defense Documentation Center Cameron Station Alexandria, VA 22314	2
2.	Library, Code 0212 Naval Postgraduate School Monterey, CA 93940	2
3.	Department Chairman, Code 52 Department of Electrical Engineering Naval Postgraduate School Monterey, CA 93940	2
4.	Assoc. Professor J. B. Knorr, Code 52Ko Department of Electrical Engineering Naval Postgraduate School Monterey, CA 93940	1
5.	Assoc. Professor R. W. Adler, Code 52Ab Department of Electrical Engineering Naval Postgraduate School Monterey, CA 93940	1
6.	LTJG Ram Sharon, Israeli Navy c/o Embassy of Israel 1621 22nd Street, N.W. Washington, D.C. 20008	2
7.	LT David Bar-Yehoshua, Israeli Navy Department of Electrical Engineering Naval Postgraduate School Monterey, CA 93940	1
8.	Defense and Armed Forces Attache' Embassy of Israel 1621-22nd Street, N.W. Washington, D.C. 20008	2

thes4347

Theoretical analysis of a model for a fi



3 2768 000 99573 2

DUDLEY KNOX LIBRARY